

# Canonicalization of Batched Einstein Summations for Tuning Retrieval

**KAUSHIK KULKARNI**, Siebel School of Computing and Data Science, University of Illinois at Urbana-Champaign, USA

**ANDREAS KLÖCKNER**, Siebel School of Computing and Data Science, University of Illinois at Urbana-Champaign, USA

We present an algorithm for normalizing *Batched Einstein Summation* expressions by mapping mathematically equivalent formulations to a unique normal form. Batches of einsums with the same Einstein notation that exhibit substantial data reuse appear frequently in finite element methods (FEM), numerical linear algebra, and computational chemistry. To effectively exploit this temporal locality for high performance, we consider groups of einsums in batched form.

Representations of equivalent batched einsums may differ due to index renaming, permutations within the batch, and, due to the commutativity and associativity of multiplication operation. The lack of a canonical representation hinders the reuse of optimization and tuning knowledge in software systems. To this end, we develop a novel encoding of batched einsums as colored graphs and apply graph canonicalization to derive a normal form.

In addition to the canonicalization algorithm, we propose a representation of einsums using functional array operands and provide a strategy to transfer transformations operating on the normal form to *functional batched einsums* that exhibit the same normal form; crucial for fusing surrounding computations for memory bound einsums. We evaluate our approach against JAX, and observe a geomean speedup of 4.7× for einsums from the TCCG benchmark suite and an FEM solver.

**CCS Concepts:** • **Applied computing** → *Physics*; • **Mathematics of computing** → **Mathematical software performance**; • **Computing methodologies** → *Representation of mathematical objects*.

Additional Key Words and Phrases: Tensor Contractions, Optimizing Compiler, Graph Isomorphism, DSL

## ACM Reference Format:

Kaushik Kulkarni and Andreas Klöckner. 2026. Canonicalization of Batched Einstein Summations for Tuning Retrieval. 1, 1 (January 2026), 37 pages. <https://doi.org/10.1145/nnnnnnnn.nnnnnnnn>

## 1 Introduction

Linear Algebra subprograms serve as an abstraction layer between performance engineers and computational scientists. The role of a performance engineer is to provide optimized kernels tailored to specific hardware architectures, while a computational scientist implements their application by composing these kernels. Well-known examples for such abstractions include BLAS [36] for primitives on dense linear operator applications, LAPACK [6] for solving linear

---

Authors' Contact Information: **Kaushik Kulkarni**, kgk2@illinois.edu, Siebel School of Computing and Data Science, University of Illinois at Urbana-Champaign, Urbana, Illinois, USA; **Andreas Klöckner**, andreask@illinois.edu, Siebel School of Computing and Data Science, University of Illinois at Urbana-Champaign, Urbana, Illinois, USA.

---

Permission to make digital or hard copies of all or part of this work for personal or classroom use is granted without fee provided that copies are not made or distributed for profit or commercial advantage and that copies bear this notice and the full citation on the first page. Copyrights for components of this work owned by others than the author(s) must be honored. Abstracting with credit is permitted. To copy otherwise, or republish, to post on servers or to redistribute to lists, requires prior specific permission and/or a fee. Request permissions from permissions@acm.org.

© 2026 Copyright held by the owner/author(s). Publication rights licensed to ACM.

Manuscript submitted to ACM

systems, PETSc [9] for iterative linear / non-linear solvers, among others. By relying on such abstractions, computational scientists can focus on formulating their applications while leveraging the optimized routines provided by the implementation of such systems to achieve performant execution on the underlying hardware systems.

A key operation observed across many scientific domains is the multilinear algebra operator application. Such operators generalize inner and outer products to multidimensional arrays and appear in a wide range of contexts. For example, expressions of the form  $\sum_{xj} J[x, r, e]D[x, i, j]u[e, j]$  appear during matrix-free assembly in Finite Element Methods (FEM) [24], expressions of the form  $\sum_{cd} g[i, j, c, d]t[c, d, a, b]$  appear in cluster operators in Computational Chemistry [48], and expressions of the form  $\sum_{j_1 j_2} G_1[i_1, j_1]G_2[i_2, j_2]X[j_1, j_2]$  appear in Tensor Train Layers in Neural Networks [41], etc. Åhlander et al. [4] proposed a Domain-Specific Language (DSL) that utilizes the Einstein Summation (“einsum”) notation as an abstraction to offer a terse syntax for expressing such multidimensional contractions. This notation has since been adopted by a number of systems that support operations on arrays, including NumPy [17], JAX [16], CYCLOPS [47], and DEINSUM [58].

In large-scale applications, einsums rarely occur in isolation; instead, they are often evaluated in groups with repeated access to the same data. For example, in FEM applications, each derivative computation corresponds to the same einsum expression applied to different field vectors, while certain operands, such as geometric factors, remain unchanged. To represent this data reuse, we find it critical to introduce a computational primitive corresponding to a collection (unordered) of einsums sharing the same Einstein notation but applied to different array operands. We use the term “batched einsum” for this concept.

The ubiquity of batched einsums in scientific workloads makes it essential to optimize their execution speed for available target hardware. Utilizing state-of-the-art compilation techniques for einsums to lower batched einsums often face two key drawbacks. Firstly, these approaches tend to lower einsums into a program by obtaining an optimal contraction path and subsequently relying on a tensor contraction code-generator [20, 23, 38, 50]. This introduces overheads from the allocation and initialization of intermediate arrays, referred to as materialization overheads. Secondly, they do not fuse the data accesses across einsum invocations leading to further overheads from DRAM-to-register reads. For these reasons, we take a contrasting approach and design a software system that maintains a tabulation of high-performant batched einsums to be reused in practical programs.

We refer to the software systems that provide a tailored implementation for an instance of a computational primitive as adopting a *tabulation-based* approach. Encoding batched einsums within such a table for retrieval poses a key challenge due to the non-canonical nature of their representation. This can lead to inefficiencies, with multiple table entries corresponding to mathematically equivalent computations. We illustrate this in Figure 1, where two syntactically different batched einsums can share the same computational implementation after appropriate renaming. In Section 5, we formalize these equivalent classes of batched einsums by considering duplicates that may arise from index renaming, permutations within a batch, and permutations of operands within an einsum. Additionally, we have developed a *canonicalization algorithm* that maps a batched einsum expression to a canonical form. This algorithm ensures that equivalent batched einsum expressions are mapped to a unique representation.

A key drawback of systems that adopt a tabulation-based approach for optimized subprograms, like BLAS, is the requirement of the operands of the computational primitive to be materialized. These materialization overheads limit the application’s computational throughput, particularly when the primitive itself is memory bound. We illustrate this in Algorithm 1, where the low arithmetic intensity of matrix-vector product makes it is generally profitable to fuse

$R_1[i, j, k, l] \leftarrow \sum_{m,n} A[m, n, j]B[m, n, i]C[k, l, i]$ $R_2[i, j, k, l] \leftarrow \sum_{m,n} D[m, n, j]E[m, n, i]A[k, l, i]$ $R_3[i, j, k, l] \leftarrow \sum_{m,n} B[m, n, j]D[m, n, i]F[k, l, i]$	$R'_1[n', m', k', j'] \leftarrow \sum_{i', l'} A'[l', i', n']D'[k', j', n']E'[l', i', m']$ $R'_2[n', m', k', j'] \leftarrow \sum_{i', l'} E'[l', i', n']B'[k', j', n']C'[l', i', m']$ $R'_3[n', m', k', j'] \leftarrow \sum_{i', l'} C'[l', i', n']F'[k', j', n']D'[l', i', m']$
--	--

(a) Batched einsum  $e_1$ .(b) Batched einsum  $e_2$ .

Fig. 1. Although  $e_1$  and  $e_2$  appear distinct set of expressions, the implementation of  $e_1$  can be utilized for computing  $e_2$  provided the following substitutions are applied to it:  $R_2 \rightarrow R'_1$ ,  $R_3 \rightarrow R'_2$ ,  $R_1 \rightarrow R'_3$ ,  $i \rightarrow n'$ ,  $j \rightarrow m'$ ,  $k \rightarrow k'$ ,  $l \rightarrow j'$ ,  $m \rightarrow l'$ ,  $n \rightarrow i'$ ,  $A \rightarrow D'$ ,  $B \rightarrow C'$ ,  $C \rightarrow F'$ ,  $D \rightarrow E'$ ,  $E \rightarrow A'$ , and  $F \rightarrow B'$ .

the computation of  $q_1$  with the BLAS' GEMV<sup>1</sup> call. Such unmaterialized array expressions appear as operands to an einsum in many scientific applications. For example, in the computation of the 1-D Coulomb interaction matrix which takes in an elementwise reciprocal of the distance matrix as an operand. Such materialization overheads also appear in high-level compilers that rely on libraries of optimized subprograms, as they are often required to aggressively materialize intermediate values in order to invoke these subprograms. This can be observed in lazy array frameworks such as JAX and PyTorch [42], which rely on dense linear algebra kernels provided by cuBLAS. In certain cases, this leads to inefficient generated binaries due to kernel boundaries that inhibit fusion.

We address these materialization-induced penalties through two key ideas. First, the computational scientist interacts with a functional form of the batched einsum expression, in which the operands of the einsum are specified as  $\lambda$ -expressions. Algorithm 2 illustrates how a computational scientist can express a computation as a *functional batched einsum*. Second, we maintain a database that records the code transformations required to optimize a *functional batched einsum* when each  $\lambda$  operand corresponds to a C-style multidimensional array. This design enables the computational scientist to reuse optimizations developed for idealized batched einsums to transform programs that structurally resemble a batched einsum. Such transfer of code optimizations is becoming increasingly important as modern accelerators, such as the NVIDIA H100, NVIDIA V100, and AMD MI250X, exhibit very high saturation arithmetic intensity. Consequently, for workloads that are memory-bound, performing additional floating-point operations on data already resident on the processing units would have virtually no impact on the execution time.

---

**Algorithm 1** Pseudocode for computing  $\nabla \cdot (\sin(q))$  using FEM.

---

```

1 procedure FEMOPERATOR( $D, q$ )
2   for  $i \in \{0, \dots, N\}$  do
3     |  $q_1[i] \leftarrow \sin(q[i])$ 
4      $y \leftarrow \text{BLASGEMV}(D, q_1)$ 
5   return  $y$ 

```

---



---

**Algorithm 2** Functional batched einsum representation for FEMOperator in Algorithm 1.

---

```

1 procedure FEMOPERATOR( $D, q$ )
2    $\lambda_A := \lambda i. j. D[i, j]$ 
3    $\lambda_x := \lambda j. \sin(q[j])$ 
4    $y \leftarrow \text{EINSUM}(ij, j \rightarrow i, \lambda_A, \lambda_x)$ 
5   return  $y$ 

```

---

We have implemented the computation of the normal form, matching of functional batched einsums to idealized batched einsums, as well as a prototype database retrieval for optimized variants in an open-source Python library, called

<sup>1</sup>GEMV corresponds to a dense matrix-vector product operation

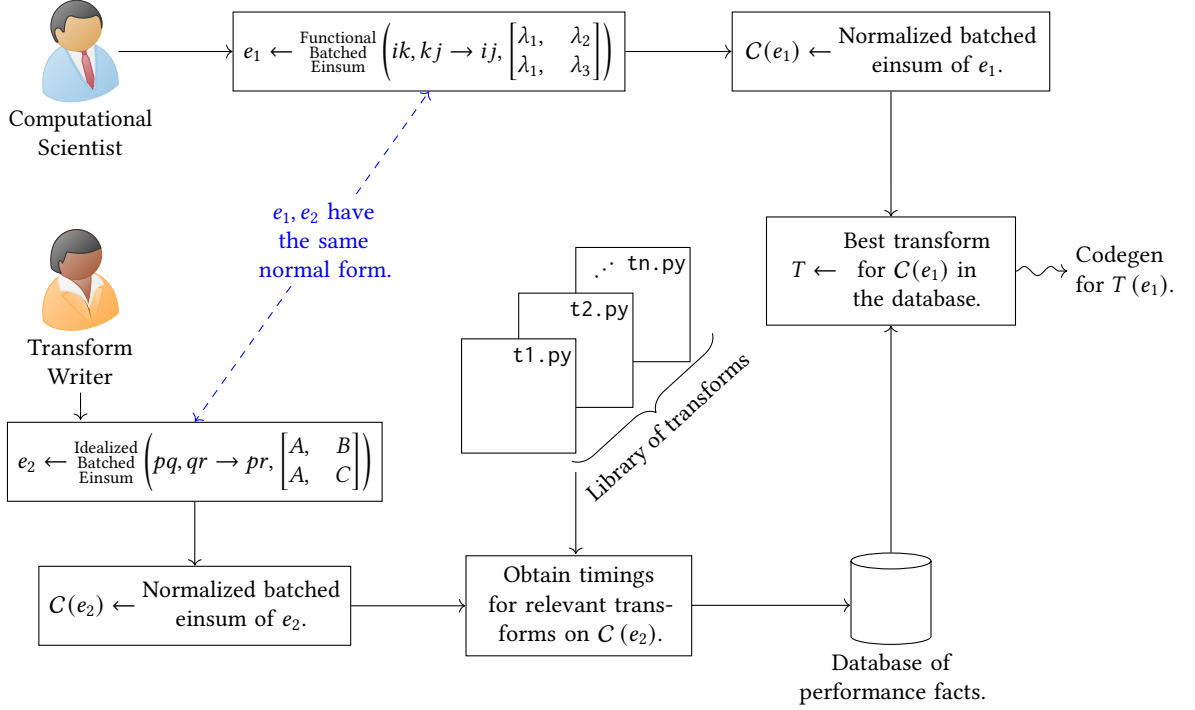


Fig. 2. The FEINSUM approach to achieve *separation of concerns*. Computational scientist expresses his workload as a functional batched einsum and retrieves optimizations from the database. Transformation writer implements transformations for idealized batched einsums and records their performance in the database. The normal form is integral in allowing the reuse of transformation knowledge from the performance engineer to the high-level programmer.

FEINSUM<sup>2</sup>. In FEINSUM, we incorporate an SQL database which maps canonical batched einsums to high-performance code-transformations on target hardware. The database enables computational scientists to straightforwardly incorporate learned transformation knowledge into their programs. Additionally, it provides valuable data points for transform writers to evaluate advanced auto-tuning approaches. In Figure 2, we see how the computation of normal form is an integral requirement for FEINSUM.

In this work, we present the following contributions:

- A definition of a computational primitive representing an unordered collection of einsum operations. We refer to this primitive as a “batched einsum”. Subprograms that perform batched einsums allow for the modeling of operand reuse between the individual einsums, providing a performance engineer to develop tailored implementations that leverage such reuse.
- A canonicalization algorithm for batched einsum expressions. The algorithm resolves the inherent ambiguities in Einstein notation arising from the commutativity of multiplication and the possibility of index renaming.
- An extension of batched einsums, called *functional batched einsums*, that considers  $\lambda$ -expressions as its operands. This facilitates the transfer of code optimizations known for idealized batched einsum instances to practical programs, especially relevant for devices with high saturation arithmetic intensity.

<sup>2</sup><https://pypi.org/project/feinsum>

- An open-source software system that implements the matching of functional batched einsums to their idealized forms and the mapping of batched einsums to a canonical form to create and manage a database. This database maps the canonical form of some instances of batched einsums to their corresponding near-optimal code transformations.

## 2 Preliminaries

### 2.1 Multidimensional Arrays

We will use the following definition of a multidimensional array.

**Definition 1.** A multidimensional array is a data type that has the following features:

**DIM** Dimensionality of the array. If  $a$  is a multidimensional array then  $\text{Dim}(a)$  evaluates to, a non-negative integer.

**SHAPE** Shape of the array. If  $a$  is a multidimensional such that  $\text{Dim}(a) = N$ , then  $\text{Shape}(a)$  evaluates to a sequence of  $N$  non-negative integers.

**DTYPE** Data type of an element of the array. If  $a$  is an array, then  $\text{Dtype}(a)$  evaluates to a numeric data type. We refer the reader to NumPy [17] for an exhaustive set of numeric-data types.

It further permits *index access* operation: if  $a$  is a multidimensional array with shape  $(d_1, d_2, \dots, d_n)$  and  $(i_1, i_2, \dots, i_n)$  is a sequence of non-negative integers such that  $i_k < d_k$  for all  $k \in \{1, \dots, n\}$ , then  $\text{IndexInto}(a, (i_1, i_2, \dots, i_n))$  yields a scalar value of the type  $\text{Dtype}(a)$ . We often use  $a[i_1, i_2, \dots, i_n]$  as a shorthand for the same indexing operation.

We now define the domain and codomain associated with an array as follows.

**Definition 2** (Array Domain). Let  $A$  be an  $n$ -dimensional array with shape  $(s_1, \dots, s_n)$ . The *domain* of  $A$ , denoted  $\text{dom}(A)$ , is the Cartesian product

$$\text{dom}(A) = \prod_{i=1}^n \{0, 1, \dots, s_i - 1\},$$

that is, the set of all valid index tuples for accessing elements of  $A$ .

**Definition 3** (Array Codomain). Let  $A$  be a multidimensional array. The *codomain* of  $A$ , denoted by  $\text{codomain}(A)$ , is the set of all scalar values of type  $\text{Dtype}(A)$ .

### 2.2 Einstein Notation

The popular Einstein summation convention [15] was developed as a notation for contraction operation over tensors. In scientific software, a slightly modified version of that definition is used for contractions over multidimensional arrays. We now introduce a grammar that permits computational representation of expressions in Einstein summation form.

**Definition 4** (Index). An *index*,  $i$  is an expression with the grammar as shown in Listing 1.

```
<index> = "a" | "b" | "c" | .. | "z"
```

Listing 1. Grammar for an index

We use the *index* expression to define an index list.

**Definition 5** (Index List). An index list  $\mathcal{I}$  is an expression built from a sequence of index expressions as shown in the grammar of Listing 2.

We use the subscript notation  $\mathcal{I}_k$  to refer to the  $k$ -th index in an index list.

```
<index_list> := <index>*
```

Listing 2. Grammar for an index list, uses the `index` terminal from Listing 1

**Definition 6** (Length of an Index List). If  $\mathcal{I} = (i_1, i_2, \dots, i_n)$  is an index list, where  $i_1, \dots, i_n$  are index expressions, then the length of  $\mathcal{I}$ , denoted by  $|\mathcal{I}|$ , is equal to  $n$ .

**Definition 7** (Einstein Summation (“einsum”)). An Einstein summation is a quadruple  $(n, \mathcal{I}^{\text{out}}, (\mathcal{A}^k)_{k=1}^n, (\mathcal{I}^{\text{in},k})_{k=1}^n)$  that denotes an expression corresponding to a multidimensional array  $R$ , such that

- $n$  is a non-negative integer corresponding to number of inputs to the expression.
- $\mathcal{I}^{\text{out}}$  is an index list, corresponding to the indexing pattern in  $R$ .
- $(\mathcal{A}_k)_{k=1}^n$  is a sequence of symbols for multidimensional arrays that form the inputs of the expression.
- $(\mathcal{I}^{\text{in},k})_{k=1}^n$  is a sequence of index lists denoting the indexing behavior in the input multidimensional arrays.
- $R$  is evaluated as:

$$R[\mathcal{I}_1^{\text{out}}, \dots, \mathcal{I}_{|\mathcal{I}^{\text{out}}|}^{\text{out}}] = \sum_{\substack{n \\ \bigcup_{j=1}^n (\mathcal{I}^{\text{in},j} \setminus \mathcal{I}^{\text{out}})}} \left( \prod_{k=1}^n \mathcal{A}^k[\mathcal{I}_1^{\text{in},k}, \dots, \mathcal{I}_{\text{Dim}(\mathcal{A}^k)}^{\text{in},k}] \right). \quad (1)$$

It can be observed that for (1) to be sound, the following properties must hold:

- For all  $k \in \{1, \dots, n\}$ ,  $|\mathcal{I}^{\text{in},k}|$  must be equal to  $\text{Dim}(\mathcal{A}^k)$ .
- $\text{Dim}(R)$  must be equal to  $|\mathcal{I}^{\text{out}}|$ .
- If  $(k_1, i_1, k_2, i_2)$  satisfy  $\mathcal{I}_{i_1}^{\text{in},k_1} = \mathcal{I}_{i_2}^{\text{in},k_2}$ , then  $(\text{Shape}(\mathcal{A}^{k_1}))_{i_1}$  must be equal to  $(\text{Shape}(\mathcal{A}^{k_2}))_{i_2}$ .
- If  $i \in \{1, \dots, |\mathcal{I}^{\text{out}}|\}$ , then  $\mathcal{I}_i^{\text{out}}$  must be a subset of  $\bigcup_{k=1}^n \{\mathcal{I}_1^{\text{in},k}, \dots, \mathcal{I}_{|\mathcal{I}^{\text{in},k}|}^{\text{in},k}\}$ .

**Example 1** (Einsum). An einsum defined by the tuple  $(2, (i, j), ((i, k), (k, j)), (A^{10 \times 4}, B^{4 \times 10}))$  corresponds to a rectangular matrix multiply operation, where the output  $R^{10 \times 10}$  is computed as:

$$R[i, j] = \sum_{k=0}^3 A[i, k] \cdot B[k, j].$$

**Definition 8** (Equality of Index Lists). We say two index lists  $\mathcal{I}$  and  $\mathcal{I}'$  are equal, i.e.  $\mathcal{I} = \mathcal{I}'$ , iff:

- $|\mathcal{I}| = |\mathcal{I}'|$ .
- For all  $k \in \{1, \dots, |\mathcal{I}|\}$ ,  $\mathcal{I}_k = \mathcal{I}'_k$ .

**Definition 9** (Equality of einsums). We say two einsums  $e_1$  defined by the tuple  $(n, \mathcal{I}^{\text{out}}, (\mathcal{I}^{\text{in},k})_{k=1}^n, (\mathcal{A}^k)_{k=1}^n)$  and  $e_2$  defined by the tuple  $(n, \mathcal{I}'^{\text{out}}, (\mathcal{I}'^{\text{in},k})_{k=1}^n, (\mathcal{A}'^k)_{k=1}^n)$  to be equal i.e.  $e_1 = e_2$ , iff:

- $\mathcal{I}^{\text{out}} = \mathcal{I}'^{\text{out}}$ .
- For all  $k \in \{1, \dots, n\}$ ,  $\mathcal{I}^{\text{in},k} = \mathcal{I}'^{\text{in},k}$ .
- For all  $k \in \{1, \dots, n\}$ ,  $\mathcal{A}^k = \mathcal{A}'^k$ .

**Definition 10** (All indices in an einsum). If  $e$  is an einsum which is defined by the tuple  $(n, \mathcal{I}^{\text{out}}, (\mathcal{I}^{\text{in},k})_{k=1}^n, (\mathcal{A}^k)_{k=1}^n)$ , then  $\mathcal{I}^{\text{all}}(e)$  denotes all the indices in the einsum’s index notation, i.e.,

$$\mathcal{I}^{\text{all}}(e) = \bigcup_{k=1}^n \mathcal{I}^{\text{in},k}.$$

### 3 Related Work

Einsums are a fundamental  $n$ -d array operation seen across various domains of scientific computing. This widespread occurrence of einsum makes it integral for scientific computing frameworks to provide a primitive for it. Early frameworks, like BLAS [36], LAPACK [6], provided abstractions to implement matrix-matrix multiplication and transposes which can be composed to perform einsums. Åhlander et al. [4, 5] embraced this idea further and developed a C++-library that provided the einsum primitive and used it in the context of high-level Partial Differential Equations (PDEs) and iterative linear solvers. Hirata et al. [20] proposed Tensor Contraction Engine (TCE), a high-level  $n$ -d array manipulation framework that employed the Einstein notation to describe quantum chemistry computations. TCE’s index notation is utilized by computational chemistry frameworks, like NWChem [52]. NumPy [17] also provides a primitive for Einstein summation and has since become widely adopted by PYTHON-based machine learning frameworks. As a result, TENSORFLOW [2], JAX [16], PyTorch [42], etc., provide the “einsum”-primitive. Vasilache et al. [54] introduced Tensor Comprehensions, a high-level DSL for expressing machine learning operations using Einstein notation, which is subsequently lowered to machine code via the polyhedral model. Rogozhnikov [46] developed an  $n$ -d array library that relies on the index notation to specify array manipulation primitives. Further, in Tensor Algebra Compiler, Kjolstad et al. [25] extended the Einstein notation to be applicable over sparse operands to map operations in Finite Element Methods (FEM), Sparse Neural Networks, etc.

The ubiquity of einsum primitive across various computational frameworks has resulted in a multitude of following work that optimize them for high performance. Optimized BLAS implementations, such as OPENBLAS [57], Intel MKL [55], BLIS [53], LIBXSMM [18], provide optimized implementations of General Matrix-matrix multiplications (GEMM). These high-performant GEMMs and transposes have been integral in early tensor contraction algorithms, such as Transpose-Transpose-GEMM-Transpose [20] (TTGT). Tensor contractions generalize matrix multiplication to multidimensional arrays and constitute a fundamental suboperation of einsums. They are typically paired with contraction path optimization algorithms to evaluate einsums in a FLOP-optimal manner. Lam et al. [13] showed that this optimization problem is NP-hard. Pfeifer et al. [43] propose a pruning strategy for the contraction path search space. Smith et al. [1] implement this search heuristic, along with others, in OPT-EINSUM, which has been subsequently used in NumPy, JAX, etc. There has also been a wide array of work that proposes domain-specific loop transformations for tensor contraction programs. We refer the reader to the work by Springer et al. [50] which includes a survey of tensor contraction approaches, such as TTGT, Loops over GEMM, and nested loops approaches. Additionally, the authors also propose GEMM-like Tensor-Tensor multiplication (GETT) that avoids materializing the transposes and performs transposition on the tiled operands which fit into the cache, which end up being as operands of a GEMM micro-kernel. Kim et al. [23] develop an algorithm for tensor contractions targeting GPUs. They prefetch the tiled operands to scratchpad memory and construct the tiled output via outer products. The prefetching and outer product computation is performed parallelly by the work-items of work-group. In TVM, Chen et al. [12] propose an auto-tuning based lowering pass that explores various loop transformations. Their simulated annealing based auto-tuner is shown to be competitive with simpler hand-tuned tensor contractions implemented in cuBLAS.

The availability of high-performance tensor contractions / einsums has also led to key applications that rely on these high-level routines. Rocktäschel [45] shows this in the context of machine-learning workloads. In a previous study [34], we demonstrated that einsums form the core operation in an end-to-end FEM timestepper. Julien et al. [26] demonstrate potential profitability of decomposing array expressions into einsums. Barthels et al. [10] present a compiler that accepts array expressions and rewrites them into optimized BLAS and LAPACK routines.

To exploit data reuse across multiple invocations of linear algebra primitives and to improve utilization of wide SIMD architectures, batched linear algebra operators have been studied. Abdelfattah et al. [3] developed an auto-tuning based strategy for generating optimized batched GEMM routines on GPU architectures. Dongarra et al. [14] employed cross-matrix vectorization to implement efficient batched GEMM and triangular solvers on wide SIMD architectures. Kim et al. [22] proposed a lowering strategy for batches of tensor contractions. In this work, we introduce a computational primitive for a collection of einsum operations, referred to as a batched einsum. Existing approaches to batching einsums typically introduce an additional index to represent the batch dimension, however, such formulations fail to capture fine-grained operand reuse and enforce arbitrary materialization constraints that results in performance degradation.

To summarize, einsums comprise a key computational construct in scientific computing codes. Many algorithms to compile einsums have been proposed, however as evident from Table 3.4 of [50], no algorithm strictly achieves roofline for all cases. Consequently, many scientific computing frameworks choose to use handwritten kernels. We see this in the context of state-of-the-art Finite Element Solvers [30, 31]. To address these issues, in this work, we propose a software framework that helps to tabulate near-roofline kernels for instances of batched einsums, while allowing the tabulated knowledge be reusable in a user-driven computational setting. A key requirement for encoding an instance of batched einsum in a table for retrieval is the ability to map it to a *normal form*. To the best of our knowledge, no prior work has addressed the problem of computing the normal form for einsum expressions, let alone batched einsums.

#### 4 Batched Einstein Summation

It is common in computational science applications to invoke a kernel corresponding to an einsum instance repeatedly, with substantial overlap in the data accessed across invocations. Such patterns arise, for example, within the *hot loops* of FEM solvers, where expressions of the form

$$\sum_{j,x} J[x, r, e] D[x, i, j] u_k[e, j], \quad k \in \{1, \dots, N_{\text{field}}\},$$

occur frequently. Here,  $J$  is the Jacobian,  $D$  is the divergence matrix associated with the reference cell and  $u_k$  the field vectors defined over a common discretization with affine geometry mapping. When these  $N_{\text{field}}$  einsums are evaluated independently, the shared operands  $J$  and  $D$  are repeatedly loaded, resulting in additional DRAM-to-processing unit traffic and degraded performance. Similar patterns arise in electronic structure calculations as well as in linear and nonlinear solvers.

To capture this, we introduce an operation that encompasses multiple einsum operations, referred to as the *Batched Einstein Summation* operator.

**Definition 11** (Batched Einstein Summation). A Batched Einstein Summation is a quintuple  $(b, n, \mathcal{I}^{\text{out}}, (\mathcal{I}^{\text{in},j})_{j=1}^n, ((\mathcal{A}^{i,j})_{j=1}^n)_{i=1}^b)$ , which evaluates a sequence of  $b$  multidimensional arrays  $(R_i)_{i=1}^b$ . Each  $R_i$  is the result of an einsum operation defined by the quadruple  $(n, \mathcal{I}^{\text{out}}, (\mathcal{I}^{\text{in},j})_{j=1}^n, (\mathcal{A}^{i,j})_{j=1}^n)$  for  $i \in \{1, 2, \dots, b\}$ .

We will now provide an example of a *batched einsum*.

**Example 2** (Batched einsum). A batched einsum defined by the tuple:

$$(2, 3, (i, j), ((i, k), (k, l), (l, j)), ((A^{10 \times 10}, B^{10 \times 10}, C^{10 \times 10}), (B^{10 \times 10}, C^{10 \times 10}, D^{10 \times 10})))$$

corresponds to the computation of arrays  $R_1^{10 \times 10}$ , and,  $R_2^{10 \times 10}$  that are evaluated as:

$$\begin{aligned} R_1[i, j] &= \sum_{k=0}^9 \sum_{l=0}^9 A[i, k] B[k, l] C[l, j], \\ R_2[i, j] &= \sum_{k=0}^9 \sum_{l=0}^9 B[i, k] C[k, l] D[l, j]. \end{aligned} \tag{2}$$

We will now define certain operations on a batched einsum that will be useful in subsequent sections.

**Definition 12** (Equality of batched einsums). Two batched einsums,  $e_1 = (b, n, \mathcal{I}^{\text{out}}, (\mathcal{I}^{\text{in},j})_{j=1}^n, ((\mathcal{A}^{i,j})_{j=1}^n)_{i=1}^b)$ , and,  $e_2 = (b, n, \mathcal{I}'^{\text{out}}, (\mathcal{I}'^{\text{in},j})_{j=1}^n, ((\mathcal{A}'^{i,j})_{j=1}^n)_{i=1}^b)$  are equal i.e.  $e_1 = e_2$ , iff for all  $i \in \{1, \dots, b\}$ , the einsums defined by  $(n, \mathcal{I}^{\text{out}}, (\mathcal{I}^{\text{in},j})_{j=1}^n, (\mathcal{A}^{i,j})_{j=1}^n)_{i=1}^b$  is equal to the einsum defined by  $(n, \mathcal{I}'^{\text{out}}, (\mathcal{I}'^{\text{in},j})_{j=1}^n, (\mathcal{A}'^{i,j})_{j=1}^n)_{i=1}^b$ .

**Definition 13** (All arguments of a batched einsum). Let  $e = (b, n, \mathcal{I}^{\text{out}}, (\mathcal{I}^{\text{in},j})_{j=1}^n, ((\mathcal{A}^{i,j})_{j=1}^n)_{i=1}^b)$  be a batched einsum, we obtain all arguments of the einsum i.e.  $\mathcal{A}^{\text{all}}(e)$  as

$$\mathcal{A}^{\text{all}}(e) = \bigcup_{i=1}^b \{\mathcal{A}^{i,1}, \dots, \mathcal{A}^{i,n}\}.$$

## 5 Isomorphic Batched Einstein Summations

In Figure 1, we highlighted the non-canonical nature of batched einsum expressions, where syntactically different batched einsum expressions can correspond to the same operation. In this section, we provide a formal definition of equivalent classes of batched einsums, which we refer to as *isomorphic batched einsums*.

First, we introduce the concept of isomorphic einsums and then use this concept to define isomorphic batched einsums.

**Definition 14** (Einsum Isomorphism). We say two einsums,  $e_1 = (n, \mathcal{I}^{\text{out}}, (\mathcal{I}^{\text{in},j})_{j=1}^n, (\mathcal{A}^j)_{j=1}^n)$ , and,  $e_2 = (n, \mathcal{I}'^{\text{out}}, (\mathcal{I}'^{\text{in},j})_{j=1}^n, (\mathcal{A}'^j)_{j=1}^n)$ , to be isomorphic i.e.  $e_1 \simeq e_2$ , if  $|\mathcal{I}^{\text{all}}(e_1)| = |\mathcal{I}^{\text{all}}(e_2)|$  and there exists three substitution mappings  $\sigma^j$ ,  $\sigma^{\mathcal{I}}$ , and,  $\sigma^{\mathcal{A}}$  such that:

- $\sigma^j : \{1, 2, \dots, n\} \rightarrow \{1, 2, \dots, n\}$  is a bijective mapping corresponding to the operand ordering between the two einsums.
- $\sigma^{\mathcal{I}} : \mathcal{I}^{\text{all}}(e_2) \rightarrow \mathcal{I}^{\text{all}}(e_1)$  is a bijective mapping corresponding to the index name mapping between the two einsums.
- $\sigma^{\mathcal{A}} : \{A'^1, \dots, A'^n\} \rightarrow \{A^1, \dots, A^n\}$  is a bijective mapping corresponding to the argument name mapping between the two einsums.
- For all  $j \in \{1, 2, \dots, n\}$ ,  $\text{Shape}(\mathcal{A}^j) = \text{Shape}(\sigma^{\mathcal{A}}(\mathcal{A}'^{\sigma^j(j)}))$  and  $\text{Dtype}(\mathcal{A}^j) = \text{Dtype}(\sigma^{\mathcal{A}}(\mathcal{A}'^{\sigma^j(j)}))$ .
- For all  $j \in \{1, 2, \dots, n\}$  and  $d \in \{1, 2, \dots, |\mathcal{I}^{d,\text{in}}|\}$ ,  $|\mathcal{I}^{\text{in},j}| = |\mathcal{I}'^{\text{in},\sigma^j(j)}|$  and  $\mathcal{I}_d^{\text{in},j} = \sigma^{\mathcal{I}}(\mathcal{I}_d'^{\text{in},\sigma^j(j)})$ .
- $|\mathcal{I}^{\text{out}}| = |\mathcal{I}'^{\text{out}}|$ .
- For all  $d \in \{1, 2, \dots, |\mathcal{I}^{\text{out}}|\}$ ,  $\mathcal{I}_d^{\text{out}} = \sigma^{\mathcal{I}}(\mathcal{I}_d'^{\text{out}})$ .

**Example 3** (Isomorphic einsums). The einsums  $e_1$  defined by the tuple  $\left(2, (i, j), ((i, k), (k, j)), (A^{10 \times 4}, B^{4 \times 10})\right)$  and  $e_2$  defined by the tuple  $\left(2, (p, q), ((r, q), (p, r)), (X^{4 \times 10}, Y^{10 \times 4})\right)$  are isomorphic with the substitution mappings:

- $\sigma^j = \{1 \mapsto 2; 2 \mapsto 1\}$ .
- $\sigma^I = \{p \mapsto i; q \mapsto j; r \mapsto k\}$ .
- $\sigma^{\mathcal{A}} = \{Y \mapsto A; X \mapsto B\}$ .

**Definition 15** (Batched einsum Isomorphism). We say two batched einsums,  $e_1 = \left(b, n, \mathcal{I}^{\text{out}}, (\mathcal{I}^{\text{in}, j})_{j=1}^n, \left((\mathcal{A}^{i, j})_{j=1}^n\right)_{i=1}^b\right)$ , and  $e_2 = \left(b, n, \mathcal{I}'^{\text{out}}, (\mathcal{I}'^{\text{in}, j})_{j=1}^n, \left((\mathcal{A}'^{i, j})_{j=1}^n\right)_{i=1}^b\right)$ , to be isomorphic i.e.  $e_1 \simeq e_2$ , if there exists four substitution mappings  $\sigma^i$ ,  $\sigma^j$ ,  $\sigma^I$  and,  $\sigma^{\mathcal{A}}$  such that:

- $\sigma^i : \{1, 2, \dots, b\} \rightarrow \{1, 2, \dots, b\}$  is a bijective mapping.
- $\sigma^{\mathcal{A}} : \mathcal{A}^{\text{all}}(e_2) \rightarrow \mathcal{A}^{\text{all}}(e_1)$  is a bijective mapping.
- For all  $i \in \{1, 2, \dots, b\}$ , the einsums defined by  $\left(n, \mathcal{I}^{\text{out}}, (\mathcal{I}^{\text{in}, j})_{j=1}^n, (\mathcal{A}^{i, j})_{j=1}^n\right)$  is isomorphic to  $\left(n, \mathcal{I}'^{\text{out}}, (\mathcal{I}'^{\text{in}, j})_{j=1}^n, \left(\mathcal{A}'^{\sigma^i(i), j}\right)_{j=1}^n\right)$  using the substitution mappings  $\sigma^j$ ,  $\sigma^I$  and  $\sigma^{\mathcal{A}}$ , where  $\sigma_i^{\mathcal{A}} = \left\{ \mathcal{A}^{i, j} \mapsto \sigma^{\mathcal{A}} \left( \mathcal{A}'^{\sigma^i(i), \sigma^j(j)} \right) : j \in \{1, \dots, n\} \right\}$ .

**Example 4** (Isomorphic batched einsums). Consider the batched einsums  $e_1$  defined by

$$(2, 4, (i), ((i, j, k), (i, k), (i, j), (i, j)), ((A^{5 \times 10 \times 10}, B^{5 \times 10}, C^{5 \times 10}, D^{5 \times 10}), (A^{5 \times 10 \times 10}, B^{5 \times 10}, C^{5 \times 10}, D^{5 \times 10}))),$$

and  $e_2$  defined by

$$(2, 4, (i), ((i, k, j), (i, k), (i, k), (i, j)), ((P^{5 \times 10 \times 10}, S^{5 \times 10}, R^{5 \times 10}, S^{5 \times 10}), (P^{5 \times 10 \times 10}, Q^{5 \times 10}, R^{5 \times 10}, S^{5 \times 10}))),$$

then  $e_1 \simeq e_2$ , using the substitution mappings:

- $\sigma^i = \{1 \mapsto 2; 2 \mapsto 1\}$ .
- $\sigma^j = \{1 \mapsto 1; 2 \mapsto 4; 3 \mapsto 3; 4 \mapsto 2\}$ .
- $\sigma^I = \{i \mapsto i; j \mapsto k; k \mapsto j\}$ .
- $\sigma^{\mathcal{A}} = \{P \mapsto A; S \mapsto B; R \mapsto C; Q \mapsto D\}$ .

## 6 A Canonical form for Batched Einsums

A direct implication of two einsums, denoted  $e_1$  and  $e_2$ , being isomorphic is that an algorithmic procedure developed for evaluating  $e_1$  can likewise be used to evaluate  $e_2$ , provided that the corresponding variables are suitably relabeled. One approach to determine if two einsums are isomorphic is by defining a *canonical form* for batched einsums such that isomorphic batched einsums have equal canonicalized representations.

**Definition 16** (Canonicalization of a batched einsum). Let  $B$  denote the set of all batched einsums. A function  $C : B \rightarrow B$  is called a *canonicalization function* if, for any batched einsum  $e$ , its canonical form  $C(e)$  satisfies

$$e \simeq e' \Leftrightarrow C(e) = C(e'),$$

for all batched einsums  $e' \in B$ .

In this section, we present one such *canonicalization function*. The procedure consists of three steps: (i) mapping a batched einsum to a colored directed graph, called the *induced graph*, (ii) canonicalizing the induced graph, and (iii) Manuscript submitted to ACM

mapping the canonicalized graph back to a batched einsum. The mappings between batched einsums and induced graphs are detailed in Appendix B.1 and Appendix B.2. We will now employ these mappings to develop a canonicalization algorithm based on colored graph canonicalization [39].

We describe our batched einsum canonicalization algorithm in the procedure `CANONICALIZEBATCHEDEINSUM` of Algorithm 3. The procedure computes  $e' = C(e)$ , together with the substitution mappings  $\sigma^{\mathcal{A}}$  and  $\sigma^{\mathcal{I}}$ . The mappings  $\sigma^{\mathcal{A}}$  and  $\sigma^{\mathcal{I}}$  map the array and index symbols of  $e'$  to their corresponding symbols in  $e$ , as specified in Definition 15.

Algorithm 3 begins by constructing an induced graph representing the batched einsum  $e$  (line 2). The components  $A$ ,  $c$ ,  $\iota_{\text{dtype}}$ ,  $\iota_{\text{length}}$ ,  $\iota_{\text{index}}$ , and  $\iota_{\text{arg}}$  correspond to the components of an induced graph as defined in Definition 24.  $A$  is the adjacency matrix corresponding to the edges in the directed graph,  $c$  is a column vector corresponding to the colors of the nodes of the graph,  $\iota_{\text{dtype}}$  is the mapping from labels of nodes corresponding to data-types in the induced graph to their numeric data types,  $\iota_{\text{length}}$  is the mapping from labels of nodes corresponding to axis lengths in the induced graph to their axis lengths, and,  $\iota_{\text{index}}$  is the mapping from labels of nodes corresponding to the indices of  $e$  to their indices.

We then invoke a graph canonicalizer to generate a relabeling map that associates the nodes of the constructed graph with their counterparts in the canonical graph. Lines 8–15 apply this relabeling map to produce the canonical form of the induced graph. At line 16, we employ the batched einsum reconstruction procedure from Appendix B.2 to obtain  $e'$ , the reconstructed batched einsum. As part of this reconstruction,  $\iota'_{\text{index}}$  and  $\iota'_{\text{arg}}$  denote the enumerations of indices and arguments selected during the process, as detailed in Step 4. and Step 5. of Appendix B.2. Finally, in lines 19–27, we construct the argument and index substitution mappings, denoted by  $\sigma^{\mathcal{A}}$  and  $\sigma^{\mathcal{I}}$ , respectively.

---

**Algorithm 3** Canonicalizing a batched einsum

---

**Require:** Procedures `INDEXNAME`, `ARGNAME`. These procedures accept a non-negative integer and deterministically return a unique index name and a unique array operand name for a batched einsum respectively. See Appendix B.2 for formal definitions.

```

1 procedure CANONICALIZEBATCHEDEINSUM( $e$ )
2    $A, c, \iota_{\text{dtype}}, \iota_{\text{length}}, \iota_{\text{index}}, \iota_{\text{arg}} \leftarrow \text{TOINDUCEDGRAPH}(e)$                                  $\triangleright$  See Appendix B.1.
3    $\text{RelabelingMap} \leftarrow \text{GETCANONLABEL}(A, c)$                                           $\triangleright$  Any graph canonization [21, 40] implementation.
4    $N \leftarrow$  # nodes in the graph corresponding to  $A$ .
5    $A' \leftarrow$  matrix of zeros of size  $N \times N$ .
6    $c' \leftarrow$  vector of zeros of size  $N$ .
7    $\iota'_{\text{dtype}}, \iota'_{\text{length}} \leftarrow$  empty map.
8   for  $i \in \{1, \dots, N\}$  do
9     for  $j \in \{1, \dots, N\}$  do
10       $| A'[\text{RelabelingMap}[i], \text{RelabelingMap}[j]] \leftarrow A[i, j]$ 
11       $| c'[\text{RelabelingMap}[i]] \leftarrow c[i]$ 
12      if  $i \in \iota_{\text{dtype}}$  then
13         $| \iota'_{\text{dtype}}[\text{RelabelingMap}[i]] \leftarrow \iota_{\text{dtype}}[i]$ 
14      if  $i \in \iota_{\text{length}}$  then
15         $| \iota'_{\text{length}}[\text{RelabelingMap}[i]] \leftarrow \iota_{\text{length}}[i]$ 
16    $e', \iota'_{\text{index}}, \iota'_{\text{arg}} \leftarrow \text{TOBATCHEDEINSUM}(A', c', \iota'_{\text{dtype}}, \iota'_{\text{length}}, \text{INDEXNAME}, \text{ARGNAME})$        $\triangleright$  See Appendix B.2.
17
18    $\sigma^{\mathcal{A}}, \sigma^{\mathcal{I}} \leftarrow$  empty maps.

```

---

---

```

19  for  $i \in \{1, \dots, N\}$  do
20    if  $i \in \iota_{\text{index}}$  then
21      oldName  $\leftarrow \iota_{\text{index}}[i]$ 
22      newName  $\leftarrow \text{IndexName}\left(\iota_{\text{index}}^{\text{inferred}}[\text{RelabelingMap}[i]]\right)$ 
23       $\sigma^I[\text{newName}] \leftarrow \text{oldName}$ 
24    if  $i \in \iota_{\text{arg}}$  then
25      oldName  $\leftarrow \iota_{\text{arg}}[i]$ 
26      newName  $\leftarrow \text{ArgName}\left(\iota_{\text{arg}}^{\text{inferred}}[\text{RelabelingMap}[i]]\right)$ 
27       $\sigma^{\mathcal{A}}[\text{newName}] \leftarrow \text{oldName}$ 
28  return  $(e', \sigma^{\mathcal{A}}, \sigma^I)$ 

```

---

REMARK 1. Since our canonicalization algorithm incorporates graph canonicalization, it satisfies the idempotence criterion, i.e. for all batched einsums  $e$ ,  $C(e) = C(C(e))$ .

**Example 5.** For the einsum  $e_1$  defined by  $(1, 2, (i), ((ij), (ik)), ((A, B)))$ , with  $\text{Shape}(A) = \text{Shape}(B) = (72, 18)$  and  $\text{Dtype}(A) = \text{Dtype}(B) = \text{F64}$ , we get  $C(e_1)$  as the batched einsum defined by  $(1, 2, (a), ((ab), (ac)), ((A_0, A_1)))$ , with  $\text{Shape}(A_0) = \text{Shape}(A_1) = (72, 18)$  and  $\text{Dtype}(A_0) = \text{Dtype}(A_1) = \text{F64}$ .

For the einsum  $e_2$  defined by  $(1, 2, (i), ((ik), (ij)), ((X, Y)))$ , with  $\text{Shape}(X) = \text{Shape}(Y) = (72, 18)$  and  $\text{Dtype}(X) = \text{Dtype}(Y) = \text{F64}$ , we get  $C(e_2)$  as the batched einsum defined by  $(1, 2, (a), ((ab), (ac)), ((A_0, A_1)))$ , with  $\text{Shape}(A_0) = \text{Shape}(A_1) = (72, 18)$  and  $\text{Dtype}(A_0) = \text{Dtype}(A_1) = \text{F64}$ . Since  $C(e_1) = C(e_2)$ ,  $e_1$  must be isomorphic to  $e_2$ .

It is worth noting that multiple canonicalization functions for batched einsums are possible. Our proposed approach relies on a graph canonicalization procedure. Furthermore, replacing the underlying graph canonicalizer in our approach with a different implementation would yield a different canonicalization function.

This canonicalization will be instrumental in tabulating batched einsums in our software system described in Section 7.

## 7 Integration of Optimized Batched Einsums into Practical Programs

In this section, we introduce our strategy for integration and practical reuse of optimized implementations of batched einsums within high-level programs. We have implemented a software system that can maintain a library of transformation plans that operate on functional batched einsums. These transformation plans are added to the library either by a performance engineer or by an autotuner. Additionally, our system maintains a database of empirically populated performance facts of the transformations in the library for specialized instances of functional batched einsums, where every function for an operand is of the form  $(i_1, \dots, i_n) \mapsto A[i_1, \dots, i_n]$ , where  $A$  is a row-major ordered multidimensional array. We refer to such instances of functional batched einsums as *idealized functional batched einsums*. A computational scientist uses these empirical facts known for idealized functional batched einsums to optimize their program that is expressed as a functional batched einsum. We have implemented this as a PYTHON library called FEINSUM<sup>3</sup>. We summarize the core components of FEINSUM and the manner in which the computational scientist and transform writer interact with it in Figure 2.

<sup>3</sup>FEINSUM is open-source and publicly available at <https://pypi.org/project/feinsum>.

A key design choice for software systems such as FEINSUM, which adopt a tabulation-based approach to provide optimized subprograms, is the structure of the computational primitive. Software systems such as BLAS, ONEDNN [37], and, LAPACK, provide the computational scientist binaries containing optimized subroutines for the computational primitives. These approaches accept operands as in-memory buffers. However, this approach of accepting buffers for operands introduces additional overheads associated with buffer allocation and initialization. We have previously observed one such instance of overheads induced by abstraction in Algorithm 1. To avoid such materialization-related overheads we extend the concept of a batched einsum such that it allows lambda expressions instead of materialized buffers as inputs. We call this a *functional batched einsum expression*. The library of transformations provided along FEINSUM operate on such functional versions of batched einsums. The database of performance facts contains measurements for an idealized version of functional batched einsums. We will now formally define functional batched einsums and the associated idealized functional batched einsum.

**Definition 17** (Functional Batched Einstein Summation). Let  $e = (b, n, \mathcal{I}^{\text{out}}, (\mathcal{I}^{\text{in},j})_{j=1}^n, ((\mathcal{A}^{i,j})_{j=1}^n)_{i=1}^b)$  be a batched einsum. Let  $\mathcal{M}$  be a mapping assigning to each  $A \in \mathcal{R}^{\text{all}}(e)$  a function

$$\mathcal{M}(A) : \text{dom}(A) \rightarrow \text{codomain}(A).$$

The *functional batched einsum* defined by the pair  $(e, \mathcal{M})$  computes a sequence of  $b$  multidimensional arrays  $(R_i)_{i=1}^b$  such that, for each  $i \in \{1, \dots, b\}$ ,

$$R_i[\mathcal{I}_1^{\text{out}}, \dots, \mathcal{I}_n^{\text{out}}] = \sum_{\bigcup_{j=1}^n (\mathcal{I}^{\text{in},j} \setminus \mathcal{I}^{\text{out}})} \left( \prod_{k=1}^n \mathcal{M}(\mathcal{A}^{i,k})(\mathcal{I}_1^{\text{in},k}, \dots, \mathcal{I}_{\text{Dim}(\mathcal{A}^k)}^{\text{in},k}) \right).$$

**Definition 18** (Idealized Functional Batched Einsum). Let  $f = (e, \mathcal{M})$  be a functional batched einsum such that

$$\mathcal{M} = \{A \mapsto \lambda i_1 \dots i_n . P_A[i_1, \dots, i_n] : A \in \mathcal{R}^{\text{all}}(e), n = \text{Dim}(A)\},$$

where  $P_A$  denotes the underlying buffer of a row-major ordered multidimensional array associated with  $A$  that is not aliased by any other array in the program. Then  $f$  is called an *idealized functional batched einsum*.

At its core, FEINSUM permits the computational scientist (or a high-level compiler) to reuse high-performant transformations known for idealized functional batched einsums to their programs resembling batched einsums. In general, the profitability analysis for the functional batched einsum is sensitive to the expressions in  $\mathcal{M}$ . Nevertheless, we argue there is a broad class of choices for  $\mathcal{M}$  that appear in real-world scenarios where transfer of such profitability analysis applies. To make this concrete, we compare the saturation arithmetic intensities of several microarchitectures with the arithmetic intensities of the einsums in the TCCG benchmark suite [49]. The results of this comparison are shown in Figure 3. We observe that, on average, 60.4% of the benchmark entries are memory bound across GPUs such as the NVIDIA P100, NVIDIA Titan V, NVIDIA H100, and AMD MI250X. A consequence of an idealized functional batched einsum being memory bound is that any functional batched einsum that performs additional computations on the operands without altering the memory access pattern exhibits similar performance characteristics. Thereby, reusing transformations developed for idealized functional batched einsums is often a suitable and effective strategy.

In our implementation of FEINSUM, we utilize the LOOPY toolkit [27]. LOOPY serves as both a language for specifying the grammar and a framework for defining the transformations on subprograms. We provide an overview of the Loopy Intermediate Representation (IR) in Appendix A. It is important to emphasize that none of the concepts introduced in this work are dependent on LOOPY. The proposed approach can be readily implemented in any high-level IR, such as

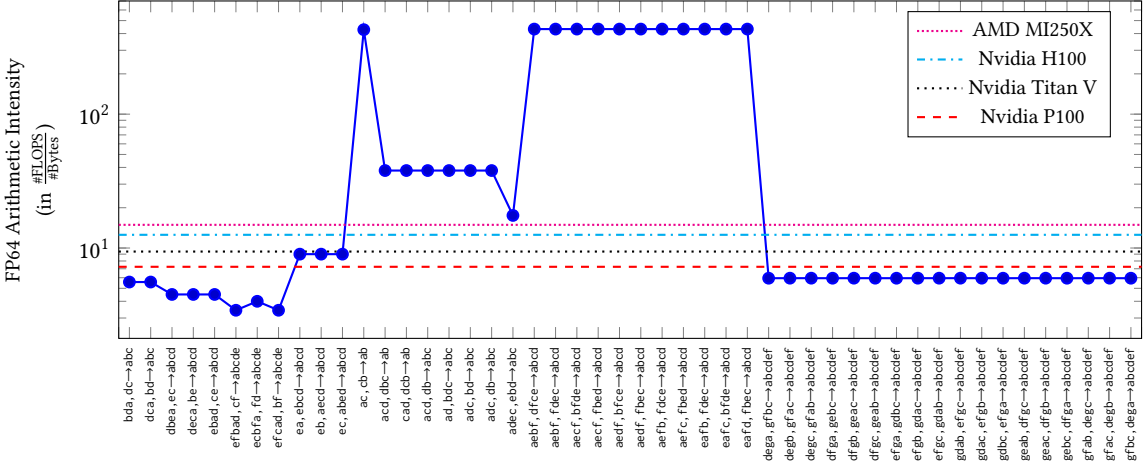


Fig. 3. Arithmetic intensities (AI) for the TCCG benchmark suite with double-precision operands. The horizontal dashed lines indicate saturation Als of modern accelerators, above which the workloads become compute-bound.

MLIR [35], TRITON [51] and HALIDE [44], provided that the representation supports abstract syntax tree (AST) nodes for expressing multidimensional arrays, loop nests and functions.

We now describe the flow shown in Figure 2 in detail using a sequence of examples. Listing 3 presents an example transformation from the transformation library. Listing 4 illustrates a retrieval from FEINSUM’s database that transforms an instance of functional batched einsum. Finally, Listing 5 shows the code generated for the retrieval in Listing 4, assuming that the transformation in Listing 3 is the best known transformation in the database. The generated code applies the library-specified transformations after computing the required substitution mappings. Moreover, the function evaluations corresponding to the operands are fused into the kernel’s inner loop.

```

1 import feinsum as fs
2 import loopy as lp
3
4 A = fs.array("A", (96, 4))
5 B, C = fs.array("B", (4,)), fs.array("C", (4,))
6 ref_ensm = fs.batched_einsum("ij, j->i", [[A, B], [A, C]])
7
8 def transform(K):
9     sigma = fs.identify_as_einsum(K, ref_ensm)
10    # Tile i-loop in chunks of 32.
11    K = lp.split_iname(K, sigma["i"], 32)
12    # Precompute "A" since it is used twice.
13    K = lp.precompute(K, sigma["A"], sweep_inames=())
14
15    return K
16
17 if __name__ == "__main__":

```

```
17  fs.record_facts(ref_ensm, device, __file__)
```

Listing 3. Transformation writer's view of `FEINSUM`. The transformation writer would implement a transformation plan targeting the kernel `K`. Here, a transformation implemented for a batched einsum corresponding to two matrix-vector multiplications as represented by `ref_ensm`.

We now examine Listing 3 in detail. The code transformation is specified in the `transform` routine, which takes as input an intermediate representation (IR) of a kernel and returns a transformed kernel. The transformation is defined for the batched einsum  $(2, 2, (i), ((ij), (j)), ((A, B), (A, C)))$ . It begins by invoking `identify_as_einsum`, which interprets the statements in the input kernel as a functional batched einsum and computes a renaming map from the variables of the reference einsum to those in the kernel IR. Interpreting lower-level IR as a higher-level operation, such as a functional batched einsum, is commonly referred to as *raising* [11]. Canonicalization is an essential component of `identify_as_einsum`; pseudocode for this procedure is provided in Algorithm 4. The resulting renaming map is then used to apply a tiling transformation (`lp.split_iname`) and to precompute the `A` operand in private memory, thereby avoiding redundant accesses to global memory. The final line of the script invokes `record_facts`, which records the runtime of the idealized functional batched einsum corresponding to `ref_ensm` after applying the `transform` routine. Before recording wall-clock times, we execute several warm-up runs on the device to mitigate transient effects. The canonical form of `ref_ensm` is used as the identifier under which these performance facts are stored.

---

**Algorithm 4** Algorithm to identify the kernel,  $K$ , as the reference einsum,  $e_{\text{ref}}$ .

---

```

1 procedure IDENTITYAsEINSUM( $K, e_{\text{ref}}$ )
2    $e_{\text{raised}}, \sigma_{\text{raised}}^{\mathcal{A}}, \sigma_{\text{raised}}^I \leftarrow \text{RAISETOBATCHEDEINSUM}(K)$ 
3    $e'_{\text{ref}}, \sigma_{\text{canon-to-ref}}^{\mathcal{A}}, \sigma_{\text{canon-to-ref}}^I \leftarrow \text{CANONICALIZEBATCHEDEINSUM}(e_{\text{ref}})$ 
4    $e'_{\text{raised}}, \sigma_{\text{canon-to-raised}}^{\mathcal{A}}, \sigma_{\text{canon-to-raised}}^I \leftarrow \text{CANONICALIZEBATCHEDEINSUM}(e_{\text{raised}})$ 
5
6   if  $e'_{\text{ref}} \neq e'_{\text{raised}}$  then
7     | Raise an exception.
8
9    $\sigma^{\mathcal{A}} \leftarrow \{\}$ 
10   $\sigma^I \leftarrow \{\}$ 
11
12  for  $a_{\text{raised}}, a_K \in \sigma_{\text{raised}}^{\mathcal{A}}$  do
13    |  $\sigma^{\mathcal{A}}[\sigma_{\text{canon-to-ref}}^{\mathcal{A}}[(\sigma_{\text{canon-to-raised}}^{\mathcal{A}})^{-1}[a_{\text{raised}}]]] \leftarrow a_K$ 
14  for  $i_{\text{raised}}, i_K \in \sigma_{\text{raised}}^I$  do
15    |  $\sigma^I[\sigma_{\text{canon-to-ref}}^I[(\sigma_{\text{canon-to-raised}}^I)^{-1}[i_{\text{raised}}]]] \leftarrow i_K$ 
```

---

```

import loopy as lp
import feinsum as fs

knl = lp.make_kernel(
    "{ [i0,i1] : 0<=i0<96 and 0<=i1<4 }",
    """
    u(i, j) := P[i, j]*P[i, j]
    v(i) := 3*cos(Q[i])+5
    w(i) := sin(R[i])
    for i0
        y1[i0] = sum([i1], u(i0, i1)*v(i1))
        y2[i0] = sum([i1], u(i0, i1)*w(i1))
    end
    """
)

transform = fs.retrieve(knl, device=...)
transformed_knl = transform(knl)

```

Listing 4. Computational scientist’s view of FEINSUM.

Querying the best performing transformation in FEINSUM’s database.

```

for (i0_out = 0; i0_out < 3; ++i0_out)
    for (i0_in = 0; i0_in < 32; ++i0_in) {
        double acc_i1 = acc_i1_0 = 0.0;
        for (int i1 = 0; i1 < 4; ++i1) {
            double p = P[i1+4*(32*i0_out+i0_in)]
                    * P[i1+4*(32*i0_out+i0_in)];
            acc_i1 += p*(3*cos(Q[i1])+5);
            acc_i1_0 += p*(sin(R[i1]));
        }
        y1[32*i0_out + i0_in] = acc_i1;
        y2[32*i0_out + i0_in] = acc_i1_0;
    }

```

Listing 5. OPENCL program for the subprogram in Listing 4 transformed as per Listing 3.

## 8 Experimental Results

In this section, we present a series of experiments designed to answer three questions. First, are there real-world scenarios where using optimized subprograms of batched einsums is profitable compared to utilizing a sequence of optimized einsum subprograms? We investigate this in Section 8.1 through a case study of batched einsum expressions arising in a Discontinuous Galerkin Finite Element Method (DG-FEM) solver. Second, is our choice of reusing optimizations for functional batched einsums relatively profitable over the traditional approach of storing executables corresponding to optimized subprograms? We examine this by evaluating the performance of the einsums from the TCCG suite [49] in Section 8.2. Finally, are the compile-time overheads introduced in our *identify-and-transform* strategy under control? We study these code generation costs for the TCCG benchmark suite in Section 8.3.

### 8.1 Batched einsums in DG-FEM Operators

Discontinuous Galerkin Finite Element Method [19] (DG-FEM) is a popular numerical method for solving Partial Differential Equations. DG-FEM is attractive because it achieves high-order accuracy on general grids while maintaining local conservation. DG-FEM maps well to GPGPUs as they have high cell-local computations and require relatively lower cross-cell communication compared to other Finite Element Methods.

Klöckner et al. [30] argue that three classes of batched einsums are primarily responsible for most computations in a DG-FEM solver. These batched einsums are:

**Face Mass Applications** These correspond to a class of kernels that can be raised to the batched einsums defined by the tuple  $(b, 3, (e, i), ((f, e), (i, f, j), (f, e, j)), ((M, J, F^k))_{k=1}^n)$ . Here,  $F^k$  are the numerical flux fields,  $M$  is the reference face mass matrix and  $J$  contains the geometry terms.  $e$  iterates over elements of the mesh,  $f$  iterates over faces of a cell,  $j$  iterates over the degrees of freedom (DOFs) of the input fields that lie on the cell's faces, and,  $i$  iterates over the output field's DOFs that lie inside the cell's volume.

We show a kernel that implements a functional form of such batched einsums in Listing 7.

**Local Divergence Computations** These correspond to a class of kernels that can be raised to the batched einsums that are defined by the tuple  $(b, 3, (e, i), ((x, r, e), (r, i, j), (e, j)), ((J, D, u^k))_{k=1}^n)$ . Here,  $u^k$  are the input fields,  $D$  is the reference derivative matrix and  $J$  contains the geometry terms.  $e$  iterates over elements of the mesh,  $x$  iterates over the topological dimension,  $r$  iterates over the spatial dimension of the ambient function space, and  $j, i$  iterate over the volume DOFs of the input and output fields respectively.

We show a kernel that implements a functional form of such batched einsums in Listing 8.

**Local Gradient Computations** These correspond to a class of kernels that satisfy can be identified as the batched einsums that are defined by the tuple  $(b, 3, (x, e, i), ((x, r, e), (r, i, j), (x, e, j)), ((J, D, u^k))_{k=1}^n)$ . Here,  $u^k$  are the fields whose local gradients are to be computed,  $D$  is the reference derivative matrix and  $J$  contains the geometry terms.  $e$  iterates over elements of the mesh,  $x$  iterates over the topological dimension,  $r$  iterates over the spatial dimension of the ambient function space, and  $i, j$  iterate over the volume DOFs of the input and output fields respectively.

We show a kernel that implements a functional form of such batched einsums in Listing 9.

We express the aforementioned batched einsums as LOOPY kernels and employ the transformations available in the default database integrated into our FEINSUM library. The transformation implementations for these batched einsum operations employ a combination of loop permutation and loop hoisting to reduce the total number of floating-point operations (FLOPs). In addition, we apply a parametric tiling strategy for the matrices  $J$  and  $D$ , together with a parametric work-group grid. Parameter tuning is performed using OPENTUNER [7]. For brevity, we omit further implementation details; interested readers are referred to Appendix C of our previous study [34] for a more comprehensive discussion.

As a baseline, we also implement the equivalent operations using JAX, a state-of-the-art array library that leverages lazy evaluation and supports operation fusion. The compilation heuristic in JAX relies on cuBLAS and cuDNN for optimized implementations for linear algebra primitives. In our JAX-based implementation, we define a PYTHON callable corresponding to the above operations and decorate it with `jax.jit` to trace the array operations within the function call.

All of our experiments were conducted on an Nvidia Titan V GPU, running the CUDA driver version 550.163. The transformed kernels are compiled using the Nvidia OPENCL kernel compiler available in the CUDA toolkit version 12.4.

Given that our evaluation aims to assess the relative profitability of our transformation strategies compared to state-of-the-art approaches, rather than conducting an absolute performance evaluation, we report the speedups achieved by the transformed kernels in comparison to the JAX version. The speedup, denoted as  $\eta$ , is calculated as follows:

$$\eta = \frac{\text{Wall-clock time for the JAX kernels}}{\text{Wall-clock time for the transformed kernels}}.$$

To avoid any transient effects, we compute the arithmetic mean of the wall-times obtained by executing each kernel multiple times. Specifically, we launch the kernel until the total wall-time spent reaches at least 2 seconds, and the kernel is invoked at least 20 times. Prior to performing the experiment for a kernel, we conduct 5 warm-up rounds to further reduce noise in the experiments.

We present the obtained speedup values in Figure 4. The charts indicate a speedup in the range of 1.6 to 100 is obtained for our suite of macro-kernels, affirming the benefits offered by our transformation abstraction over the state-of-the-art approaches. We expect higher speedup values as the number of einsums in a batched einsum increases, as relatively this leads to higher cost savings in loading the data on the GPU’s DRAM. However, it should be noted that this trend is not consistently observed in the data. This is primarily because our database does not contain all the transformations capable of achieving roofline-level performance for every einsum operation, thereby deviating from the ideal trend.

This experiment supports our claim that using batched einsums as a primitive allows the computational implementation to deliver higher performance by hiding latency corresponding to the memory accesses of operands shared across the einsums.

## 8.2 TCCG Benchmark suite with Unmaterialized Operands

Springer et al. [49] compiled a series of 48 tensor contractions seen across a broad range of use cases such as electronic structure computations, coupled cluster theory, and quantum chemistry. To model a real world scenario, we propose a slight extension to the benchmark suite, where instead of the operands to the tensor contractions being materialized operands we consider the operands be linear polynomials of arrays in memory. Specifically, instead of evaluating the performance of tensor contractions with the arrays  $A$  and  $B$ , we evaluate the performance of the tensor contraction with the operands,  $(\alpha_1 A + \beta_1)$  and  $(\alpha_2 B + \beta_2)$ , where  $\alpha_1, \alpha_2, \beta_1, \beta_2$  are scalars only known at runtime. In all our benchmarks,  $\alpha_1, \alpha_2, \beta_1$ , and  $\beta_2$  are double-precision scalars and  $A$  and  $B$  are multidimensional arrays that have double-precision entries.

For each test case in the test suite, we report the FLOP throughput as

$$\frac{\text{FLOPS in the contraction from OPT-EINSUM} + \text{FLOPS for computing } \alpha_1 A + \beta_1 \text{ and } \alpha_2 B + \beta_2}{t_{\text{wall}}},$$

where  $t_{\text{wall}}$  is the averaged wall-clock time spent in the kernel. To obtain  $t_{\text{wall}}$ , we perform 5 warmup rounds and use the arithmetic mean of wall-time for the execution of next  $N$  rounds, where  $N$  is the smallest number greater than 20 such that the aggregate wall-time spent inside the kernel is at least 2 seconds. We perform these tests on an Nvidia Titan V GPU, running the CUDA driver version 550.163. The transformed kernels are compiled using the Nvidia OPENCL kernel compiler available in the CUDA toolkit version 12.4.

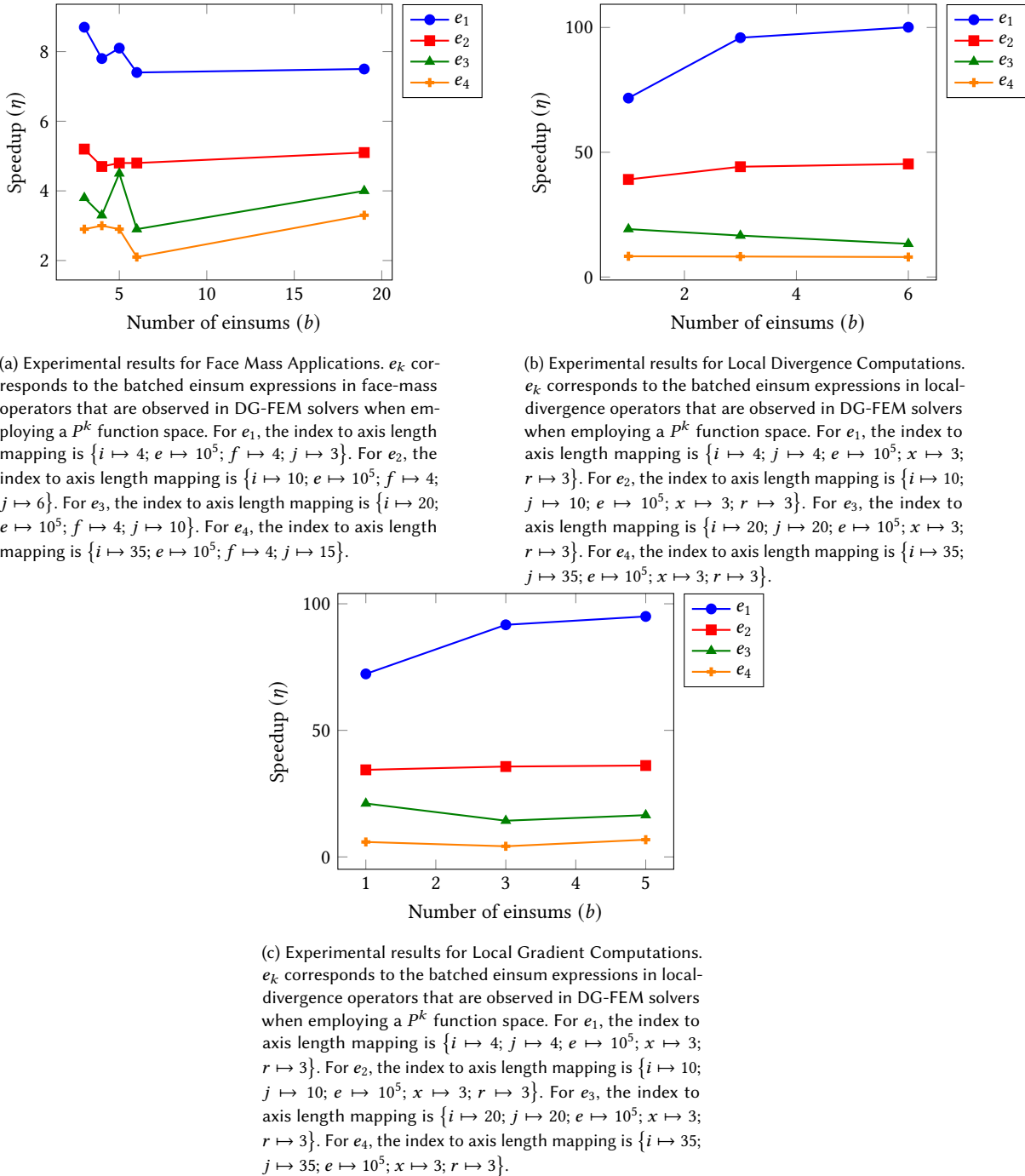


Fig. 4. Observed Speedups for batched einsums executed using `FEINSUM` relative to equivalent implementation using `JAX/`.

We also report the roofline performance [56] via a conservative model assuming that the GPU is a latency hiding machine whose performance can be limited either by the execution units or memory units. Hence, we arrive at:

$$\text{Roofline FLOPS} = \min(\text{Peak FLOPS}, \frac{\text{Total FLOPS}}{\# \text{Footprint Bytes}} \cdot \text{Peak Bandwidth}).$$

We use the manufacturer-reported values for peak FLOPS and bandwidth values.

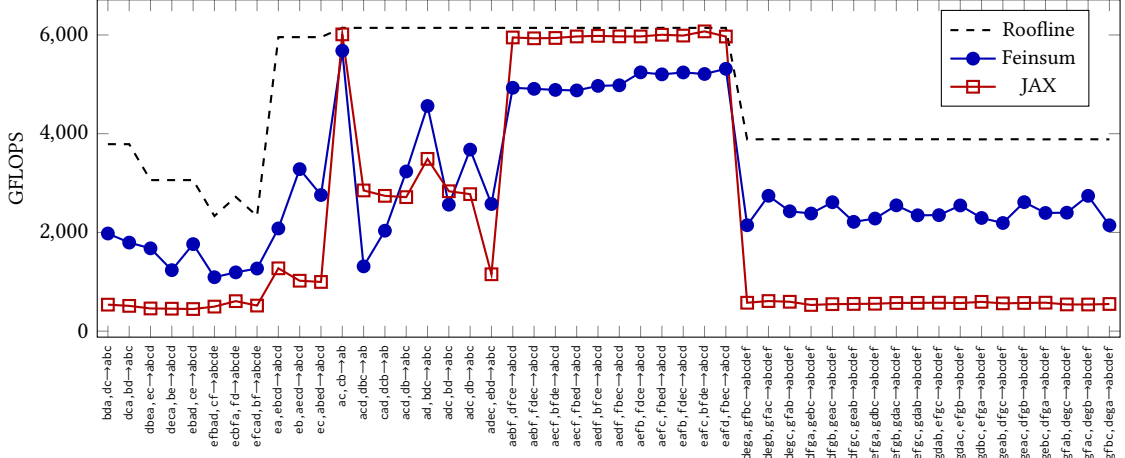


Fig. 5. FP64 FLOP throughput for the benchmarks based on the TCCG-suite as detailed in Section 8.2.

We present the data from these experiments in Figure 5. It can be observed that our transformation database contains entries that deliver 2.1× geometric-mean speedup over JAX for the TCCG suite. We attribute this speedup to two key reasons. First, JAX uses a transformation strategy similar to TTGT [20] and relies on the matrix-multiply operation available in cuBLAS, and our transformation database contains entries based on TTGT and the COGENT [23] transformation space. COGENT was previously shown to be profitable over TTGT in a geometric mean sense. Second, our *identify-and-transform* strategy couples that with fusing surrounding computations for the operands. For memory bound test-cases, cost of the actual floating point should not be apparent in wall-clock timings. This is evident by the fact that the relative speedup of our work over JAX is 3.6× for the memory-bound cases of Figure 3.

This experiment validates our claim that the reliance of widely used array compilers on BLAS primitives significantly limits their performance of tensor contraction expressions in practical programs. Meanwhile, our effort to tabulate optimized transformations for idealized batched einsums shows substantial cost reductions across this benchmark suite.

### 8.3 Time to canonicalize a batched einsum

We also aim to analyze the cost associated with the transformations, which is not accounted for in the kernel execution time. While these overheads are observed during the compilation of a larger program whose executable is reused multiple times, high compile times overheads can potentially impact the practicality of the proposed system. In our approach, these overheads include the batched einsum canonicalization process and the AST traversal for matching an einsum. Among these operations, matching an expression involves inexpensive AST traversals. However, batched einsum canonicalization relies on graph canonicalization, which exhibits sub-exponential complexity in terms of the

number of nodes in the graph. This motivates us to conduct another series of studies to quantify the expenses incurred during the canonicalization process.

In Figure 6, we present the wall-clock times required to canonicalize an instance of each einsum in the TCCG benchmark. These experiments were conducted on an AMD Ryzen 7 5800HS CPU. Across the benchmark suite, we consistently observe that the canonicalization process takes less than 1 millisecond.

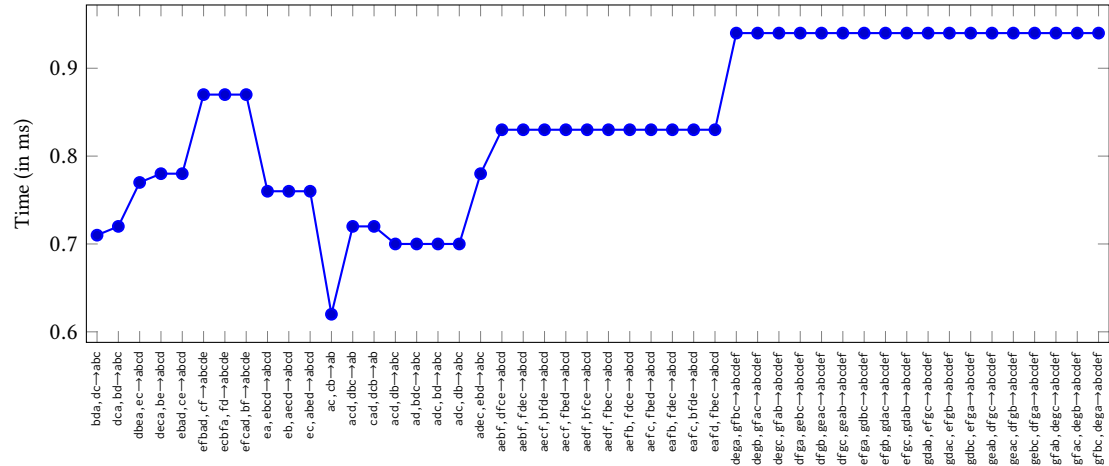


Fig. 6. Canonicalization costs for the TCCG benchmark suite.

## 8.4 Code Availability

To ensure reproducibility, we provide a DOI for an archived version of the software used to generate the results presented in this article. The software toolkit containing the canonicalization algorithm from Section 6 and an implementation of the abstraction of Section 7 have been provided as `PYTHON` library which have been archived on Zenodo [32] at the versions studied here. Similarly, the software utilized to obtain the empirical data in Section 8 has been archived on Zenodo [33]. Detailed installation instructions are provided in the `README` file included in the archived records. All contents of the archive are distributed under the MIT License.

## 9 Conclusions

In this work, we have presented three contributions. First, we have proposed an extension to the einsum computational primitive to support batches of them. Batching is an important and a commonly overlooked aspect in the synthesis of efficient code for dense linear-algebra programs. We have provided a series of experiments in the context of real-world applications to support this claim. Second, we generalize the concept of batched einsums to a formulation that accepts functions as operands, thereby facilitating operator fusion for optimizations known from their idealized versions. The case study on a modified TCCG benchmark suite has highlighted the need for such techniques in efficient handling of memory bound batched einsums. Finally, we have implemented an open-source software system that leverages the aforementioned abstractions to maintain a database of optimized code-transformations for the class of batched einsum expressions.

This work leads to some interesting questions for future research.

**Is there an einsum canonicalization algorithm with polynomial complexity?** In this work, we use graph canonicalization as an intermediate step for the canonicalization of einsums. However, an algorithm for graph canonicalization with a worst-case bound on asymptotic complexity that is polynomial is currently unavailable. One possibility is to employ Babai et al.’s [8] graph canonicalization algorithm to achieve an algorithm with quasi-polynomial complexity. However, it remains an open question whether an einsum canonicalization algorithm exists that does not rely on graph canonicalization as an intermediate step.

**What is the tight upper bound for the performance of an einsum expression?** A roofline model specific to the class of batched einsums is currently unavailable. The performance of einsum-like expressions depends on the device’s memory hierarchy, as the same memory location is accessed multiple times. This makes it challenging to develop a model that accounts for all possible bottlenecks, including L1 cache and local memory. While obtaining a model based on global memory bandwidth is relatively straightforward, it does not capture all the performance considerations in this context. Such a model could be helpful to transform writers to inform them on when to expect a tuning process to yield diminishing returns.

### Acknowledgments

The authors’ research was funded by the US National Science Foundation under awards SHF-1911019 and OAC-1931577, by the US Department of Energy under award number DE-NA0003963, as well as by the Siebel School of Computing and Data Science at the University of Illinois at Urbana-Champaign. Any opinions, findings, and conclusions, or recommendations expressed in this article are those of the authors and do not necessarily reflect the views of the sponsors; the sponsors have not approved or endorsed its content.

### References

- [1] Daniel G. a. Smith and Johnnie Gray. 2018. opt\_einsum - A Python package for optimizing contraction order for einsum-like expressions. *Journal of Open Source Software* 3, 26 (2018), 753. [doi:10.21105/joss.00753](https://doi.org/10.21105/joss.00753)
- [2] Martín Abadi, Ashish Agarwal, Paul Barham, Eugene Brevdo, Zhifeng Chen, Craig Citro, Greg S Corrado, Andy Davis, Jeffrey Dean, Matthieu Devin, et al. 2015. TensorFlow: Large-scale machine learning on heterogeneous systems.
- [3] Ahmad Abdelfattah, Azzam Haidar, Stanimire Tomov, and Jack Dongarra. 2016. Performance, Design, and Autotuning of Batched GEMM for GPUs. In *High Performance Computing*. Springer International Publishing, Cham, 21–38. [doi:10.1007/978-3-319-41321-1\\_2](https://doi.org/10.1007/978-3-319-41321-1_2)
- [4] Krister Åhlander. 2002. Einstein summation for multidimensional arrays. *Computers & Mathematics with Applications* 44, 8-9 (2002), 1007–1017.
- [5] Krister Åhlander and Kurt Otto. 2002. On software support for finite difference schemes based on index notation. In *International Conference on Computational Science*. Springer, 711–718.
- [6] Edward Anderson, Zhaojun Bai, Christian Bischof, L Susan Blackford, James Demmel, Jack Dongarra, Jeremy Du Croz, Anne Greenbaum, Sven Hammarling, Alan McKenney, et al. 1999. *LAPACK users’ guide*. SIAM.
- [7] Jason Ansel, Shoaib Kamil, Kalyan Veeramachaneni, Jonathan Ragan-Kelley, Jeffrey Bosboom, Una-May O’Reilly, and Saman Amarasinghe. 2014. OpenTuner: an extensible framework for program autotuning. In *Proceedings of the 23rd International Conference on Parallel Architectures and Compilation* (Edmonton, AB, Canada) (PACT ’14). Association for Computing Machinery, New York, NY, USA, 303–316. [doi:10.1145/2628071.2628092](https://doi.org/10.1145/2628071.2628092)
- [8] László Babai. 2019. Canonical form for graphs in quasipolynomial time: preliminary report. In *Proceedings of the 51st Annual ACM SIGACT Symposium on Theory of Computing*. 1237–1246.
- [9] Satish Balay, Kris Buschelman, William D Gropp, Dinesh Kaushik, Matthew G Knepley, L Curfman McInnes, Barry F Smith, and Hong Zhang. 2001. PETSc. See <http://www.mcs.anl.gov/petsc> (2001).
- [10] Henrik Barthels, Christos Psarras, and Paolo Bientinesi. 2021. Linnea: Automatic Generation of Efficient Linear Algebra Programs. *ACM Trans. Math. Softw.* 47, 3, Article 22 (June 2021), 26 pages. [doi:10.1145/3446632](https://doi.org/10.1145/3446632)
- [11] Lorenzo Chelini, Andi Drebes, Oleksandr Zinenko, Albert Cohen, Nicolas Vasilache, Tobias Grosser, and Henk Corporaal. 2021. Progressive Raising in Multi-level IR. In *2021 IEEE/ACM International Symposium on Code Generation and Optimization (CGO)*. 15–26. [doi:10.1109/CGO51591.2021.9370332](https://doi.org/10.1109/CGO51591.2021.9370332)
- [12] Tianqi Chen, Thierry Moreau, Ziheng Jiang, Lianmin Zheng, Eddie Yan, Haichen Shen, Meghan Cowan, Leyuan Wang, Yuwei Hu, Luis Ceze, Carlos Guestrin, and Arvind Krishnamurthy. 2018. TVM: An Automated End-to-End Optimizing Compiler for Deep Learning. In *13th USENIX Symposium on Operating Systems Design and Implementation (OSDI 18)*. USENIX Association, Carlsbad, CA, 578–594. <https://www.usenix.org/conference/osdi18/presentation/chen>

- [13] Lam Chi-Chung, P. Sadayappan, and Raphael Wenger. 1997. On Optimizing a Class of Multi-Dimensional Loops with Reduction for Parallel Execution. *Parallel Processing Letters* 07, 02 (1997), 157–168. doi:10.1142/S0129626497000176 arXiv:<https://doi.org/10.1142/S0129626497000176>
- [14] Jack Dongarra, Sven Hammarling, Nicholas J. Higham, Samuel D. Relton, and Mawussi Zounon. 2017. Optimized Batched Linear Algebra for Modern Architectures. In *Euro-Par 2017: Parallel Processing*. Springer International Publishing, Cham, 511–522. doi:10.1007/978-3-319-64203-1\_37
- [15] Albert Einstein. 1922. *The basis of the general theory of relativity*. Vol. 49. JA Barth.
- [16] Roy Frostig, Matthew James Johnson, and Chris Leary. 2018. Compiling machine learning programs via high-level tracing. *Systems for Machine Learning* 4, 9 (2018).
- [17] Charles R Harris, K Jarrod Millman, Stéfan J Van Der Walt, Ralf Gommers, Pauli Virtanen, David Cournapeau, Eric Wieser, Julian Taylor, Sebastian Berg, Nathaniel J Smith, et al. 2020. Array programming with NumPy. *Nature* 585, 7825 (2020), 357–362.
- [18] Alexander Heinecke, Greg Henry, Maxwell Hutchinson, and Hans Pabst. 2016. LIBXSMM: Accelerating Small Matrix Multiplications by Runtime Code Generation. In *SC '16: Proceedings of the International Conference for High Performance Computing, Networking, Storage and Analysis*. 981–991. doi:10.1109/SC.2016.83
- [19] Jan Hesthaven and Tim Warburton. 2007. *Nodal Discontinuous Galerkin Methods* (1 ed.). Springer New York, NY, USA. doi:10.1007/978-0-387-72067-8
- [20] So Hirata. 2003. Tensor contraction engine: Abstraction and automated parallel implementation of configuration-interaction, coupled-cluster, and many-body perturbation theories. *The Journal of Physical Chemistry A* 107, 46 (2003), 9887–9897.
- [21] Tommi Junttila and Petteri Kaski. 2011. Conflict Propagation and Component Recursion for Canonical Labeling. In *Theory and Practice of Algorithms in (Computer) Systems*, Alberto Marchetti-Spaccamela and Michael Segal (Eds.). Springer Berlin Heidelberg, Berlin, Heidelberg, 151–162. doi:10.1007/978-3-642-19754-3\_16
- [22] Jinsung Kim, Aravind Sukumaran-Rajam, Changwan Hong, Ajay Panyala, Rohit Kumar Srivastava, Sriram Krishnamoorthy, and P. Sadayappan. 2018. Optimizing Tensor Contractions in CCSD(T) for Efficient Execution on GPUs. In *Proceedings of the 2018 International Conference on Supercomputing* (Beijing, China) (ICS '18). Association for Computing Machinery, New York, NY, USA, 96–106. doi:10.1145/3205289.3205296
- [23] Jinsung Kim, Aravind Sukumaran-Rajam, Vineeth Thumma, Sriram Krishnamoorthy, Ajay Panyala, Louis-Noël Pouchet, Atanas Rountev, and Ponnuswamy Sadayappan. 2019. A code generator for high-performance tensor contractions on GPUs. In *2019 IEEE/ACM International Symposium on Code Generation and Optimization (CGO)*. IEEE, 85–95.
- [24] Robert C Kirby. 2006. Optimizing FIAT with level 3 BLAS. *ACM Transactions on Mathematical Software (TOMS)* 32, 2 (2006), 223–235.
- [25] Fredrik Kjolstad, Shoaib Kamil, Stephen Chou, David Lugato, and Saman Amarasinghe. 2017. The tensor algebra compiler. *Proc. ACM Program. Lang.* 1, OOPSLA, Article 77 (Oct. 2017), 29 pages. doi:10.1145/3133901
- [26] Julien Klaus, Mark Blacher, and Joachim Giesen. 2023. Compiling Tensor Expressions into Einsum. In *Computational Science – ICCS 2023*, Jiří Mikyška, Clélia de Mula, Maciej Paszynski, Valeria V. Krzhizhanovskaya, Jack J. Dongarra, and Peter M.A. Sloot (Eds.). Springer Nature Switzerland, Cham, 129–136.
- [27] Andreas Klöckner. 2014. Loo. py: transformation-based code generation for GPUs and CPUs. In *Proceedings of ACM SIGPLAN international workshop on libraries, languages, and compilers for array programming*. 82–87.
- [28] Andreas Klöckner. 2015. LooPy: From Fortran to Performance via Transformation and Substitution Rules. In *Proceedings of the 2nd ACM SIGPLAN International Workshop on Libraries, Languages, and Compilers for Array Programming* (Portland, OR, USA) (ARRAY 2015). Association for Computing Machinery, New York, NY, USA, 1–6. doi:10.1145/2774959.2774969
- [29] Andreas Klöckner, Lucas C. Wilcox, and T. Warburton. 2016. Array Program Transformation with LooPy by Example: High-Order Finite Elements. In *Proceedings of the 3rd ACM SIGPLAN International Workshop on Libraries, Languages, and Compilers for Array Programming* (Santa Barbara, CA, USA) (ARRAY 2016). Association for Computing Machinery, New York, NY, USA, 9–16. doi:10.1145/2935323.2935325
- [30] A. Klöckner, T. Warburton, J. Bridge, and J.S. Hesthaven. 2009. Nodal discontinuous Galerkin methods on graphics processors. *J. Comput. Phys.* 228, 21 (2009), 7863–7882. doi:10.1016/j.jcp.2009.06.041
- [31] Martin Kronbichler and Katharina Kormann. 2019. Fast Matrix-Free Evaluation of Discontinuous Galerkin Finite Element Operators. *ACM Trans. Math. Softw.* 45, 3, Article 29 (Aug. 2019), 40 pages. doi:10.1145/3325864
- [32] Kaushik Kulkarni. 2026. *Feinsum*. doi:10.5281/zenodo.1828508
- [33] Kaushik Kulkarni. 2026. *Feinsum Evaluation Artifacts*. doi:10.5281/zenodo.18285105
- [34] Kaushik G Kulkarni. 2023. *Domain-Specific Code Transformations for Computational Science based on the Polyhedral Model*. Ph.D. Dissertation. University of Illinois at Urbana-Champaign.
- [35] Chris Lattner, Mehdi Amini, Uday Bondhugula, Albert Cohen, Andy Davis, Jacques Pienaar, River Riddle, Tatiana Shpeisman, Nicolas Vasilache, and Oleksandr Zinenko. 2021. MLIR: Scaling Compiler Infrastructure for Domain Specific Computation. In *2021 IEEE/ACM International Symposium on Code Generation and Optimization (CGO)*. 2–14. doi:10.1109/CGO51591.2021.9370308
- [36] Chuck L Lawson, Richard J. Hanson, David R Kincaid, and Fred T. Krogh. 1979. Basic linear algebra subprograms for Fortran usage. *ACM Transactions on Mathematical Software (TOMS)* 5, 3 (1979), 308–323.
- [37] Jianhui Li, Zhennan Qin, Yijie Mei, Jingze Cui, Yunfei Song, Ciyong Chen, Yifei Zhang, Longsheng Du, Xianhang Cheng, Baihui Jin, Yan Zhang, Jason Ye, Eric Lin, and Dan Lavery. 2024. oneDNN Graph Compiler: A Hybrid Approach for High-Performance Deep Learning Compilation. In *2024 IEEE/ACM International Symposium on Code Generation and Optimization (CGO)*. 460–470. doi:10.1109/CGO57630.2024.10444871
- [38] Devin A Matthews. 2018. High-performance tensor contraction without transposition. *SIAM Journal on Scientific Computing* 40, 1 (2018), C1–C24.
- [39] Brendan D McKay et al. 1981. Practical graph isomorphism. (1981).

- [40] Brendan D McKay and Adolfo Piperno. 2014. Practical graph isomorphism, II. *Journal of symbolic computation* 60 (2014), 94–112.
- [41] Alexander Novikov, Dmitrii Podoprikhin, Anton Osokin, and Dmitry P Vetrov. 2015. Tensorizing Neural Networks. In *Advances in Neural Information Processing Systems*, C. Cortes, N. Lawrence, D. Lee, M. Sugiyama, and R. Garnett (Eds.), Vol. 28. Curran Associates, Inc. [doi:10.48550/arXiv.1509.06569](https://doi.org/10.48550/arXiv.1509.06569)
- [42] Adam Paszke, Sam Gross, Francisco Massa, Adam Lerer, James Bradbury, Gregory Chanan, Trevor Killeen, Zeming Lin, Natalia Gimelshein, Luca Antiga, Alban Desmaison, Andreas Kopf, Edward Yang, Zachary DeVito, Martin Raison, Alykhan Tejani, Sasank Chilamkurthy, Benoit Steiner, Lu Fang, Junjie Bai, and Soumith Chintala. 2019. PyTorch: An Imperative Style, High-Performance Deep Learning Library. In *Advances in Neural Information Processing Systems*, H. Wallach, H. Larochelle, A. Beygelzimer, F. d’Alché-Buc, E. Fox, and R. Garnett (Eds.), Vol. 32. Curran Associates, Inc. [https://proceedings.neurips.cc/paper\\_files/paper/2019/file/bdbca288fee7f92f2bfa9f7012727740-Paper.pdf](https://proceedings.neurips.cc/paper_files/paper/2019/file/bdbca288fee7f92f2bfa9f7012727740-Paper.pdf)
- [43] Robert N. C. Pfeiffer, Jutha Haegeman, and Frank Verstraete. 2014. Faster identification of optimal contraction sequences for tensor networks. *Phys. Rev. E* 90 (Sep 2014), 033315. Issue 3. [doi:10.1103/PhysRevE.90.033315](https://doi.org/10.1103/PhysRevE.90.033315)
- [44] Jonathan Ragan-Kelley, Connelly Barnes, Andrew Adams, Sylvain Paris, Frédo Durand, and Saman Amarasinghe. 2013. Halide: A Language and Compiler for Optimizing Parallelism, Locality, and Recomputation in Image Processing Pipelines. In *Proceedings of the 34th ACM SIGPLAN Conference on Programming Language Design and Implementation* (Seattle, Washington, USA) (PLDI ’13). Association for Computing Machinery, New York, NY, USA, 519–530. [doi:10.1145/2491956.2462176](https://doi.org/10.1145/2491956.2462176)
- [45] Tim Rocktäschel. 2018. Einsum Is All You Need - Einstein Summation in Deep Learning.
- [46] Alex Rogozhnikov. 2022. Einops: Clear and Reliable Tensor Manipulations with Einstein-like Notation. In *International Conference on Learning Representations*. <https://openreview.net/forum?id=oapKSVM2bcj>
- [47] Edgar Solomonik, Devin Matthews, Jeff Hammond, and James Demmel. 2013. Cyclops tensor framework: Reducing communication and eliminating load imbalance in massively parallel contractions. In *2013 IEEE 27th International Symposium on Parallel and Distributed Processing*. IEEE, 813–824.
- [48] Edgar Solomonik, Devin Matthews, Jeff R Hammond, John F Stanton, and James Demmel. 2014. A massively parallel tensor contraction framework for coupled-cluster computations. *J. Parallel and Distrib. Comput.* 74, 12 (2014), 3176–3190.
- [49] Paul Springer and Paolo Bientinesi. 2016. Design of a high-performance GEMM-like Tensor-Tensor Multiplication. *CoRR* (2016). arXiv:1607.00145 [quant-ph] <http://arxiv.org/abs/1607.00145>
- [50] Paul Springer and Paolo Bientinesi. 2018. Design of a High-Performance GEMM-like Tensor-Tensor Multiplication. *ACM Trans. Math. Softw.* 44, 3, Article 28 (Jan. 2018), 29 pages. [doi:10.1145/3157733](https://doi.org/10.1145/3157733)
- [51] Philippe Tillet, H. T. Kung, and David Cox. 2019. Triton: An Intermediate Language and Compiler for Tiled Neural Network Computations. In *Proceedings of the 3rd ACM SIGPLAN International Workshop on Machine Learning and Programming Languages* (Phoenix, AZ, USA) (MAPL 2019). Association for Computing Machinery, New York, NY, USA, 10–19. [doi:10.1145/3315508.3329973](https://doi.org/10.1145/3315508.3329973)
- [52] M. Valiev, E.J. Bylaska, N. Govind, K. Kowalski, T.P. Straatsma, H.J.J. Van Dam, D. Wang, J. Nieplocha, E. Apra, T.L. Windus, and W.A. de Jong. 2010. NWChem: A comprehensive and scalable open-source solution for large scale molecular simulations. *Computer Physics Communications* 181, 9 (2010), 1477–1489. [doi:10.1016/j.cpc.2010.04.018](https://doi.org/10.1016/j.cpc.2010.04.018)
- [53] Field G. Van Zee and Robert A. van de Geijn. 2015. BLIS: A Framework for Rapidly Instantiating BLAS Functionality. *ACM Trans. Math. Softw.* 41, 3, Article 14 (June 2015), 33 pages. [doi:10.1145/2764454](https://doi.org/10.1145/2764454)
- [54] Nicolas Vasilache, Oleksandr Zinenko, Theodoros Theodoridis, Priya Goyal, Zachary DeVito, William S. Moses, Sven Verdoolaege, Andrew Adams, and Albert Cohen. 2018. Tensor Comprehensions: Framework-Agnostic High-Performance Machine Learning Abstractions. *arXiv e-prints*, Article arXiv:1802.04730 (Feb. 2018), arXiv:1802.04730 pages. [doi:10.48550/arXiv.1802.04730](https://doi.org/10.48550/arXiv.1802.04730) arXiv:1802.04730 [cs.PL]
- [55] Endong Wang, Qing Zhang, Bo Shen, Guangyong Zhang, Xiaowei Lu, Qing Wu, and Yajuan Wang. 2014. *Intel Math Kernel Library*. Springer International Publishing, Cham, 167–188. [doi:10.1007/978-3-319-06486-4\\_7](https://doi.org/10.1007/978-3-319-06486-4_7)
- [56] Samuel Williams, Andrew Waterman, and David Patterson. 2009. Roofline: An Insightful Visual Performance Model for Multicore Architectures. *Commun. ACM* 52, 4 (April 2009), 65–76. [doi:10.1145/1498765.1498785](https://doi.org/10.1145/1498765.1498785)
- [57] Zhang Xianyi, Wang Qian, and Zhang Yunquan. 2012. Model-driven Level 3 BLAS Performance Optimization on Loongson 3A Processor. In *2012 IEEE 18th International Conference on Parallel and Distributed Systems*. 684–691. [doi:10.1109/ICPADS.2012.97](https://doi.org/10.1109/ICPADS.2012.97)
- [58] Alexandros Nikolaos Ziogas, Grzegorz Kwasniewski, Tal Ben-Nun, Timo Schneider, and Torsten Hoefler. 2022. Deinsum: Practically I/O optimal multilinear algebra. *arXiv preprint arXiv:2206.08301* (2022).

## A An overview of Loopy Intermediate Representation

Loopy Intermediate Representation (IR), introduced by Klöckner et al. [27], is a mid-level IR for modeling and transforming array-based programs. In the Loopy IR, a key data structure is the *kernel*, which consists of multiple statements executed within a polyhedrally defined iteration domain. These statements operate on arrays with specific memory layouts, data types, and address spaces. Additionally, a Loopy kernel encodes a dependence graph among the statements, which provides a partial specification of the dependencies. We present an example of a Loopy kernel in Listing 6.

```

1      ARGUMENTS:
2      A: dtype: float64, shape: (n, n)
3      n: ValueArg, dtype: int32
4      x: dtype: float64, shape: (n)
5      y1: dtype: float64, shape: (n)
6      y2: dtype: float64, shape: (n)
7
8      DOMAINS:
9      [n] -> { [i, j] : 0 <= i, j < n }
10
11     SUBSTITUTION RULES:
12     u1(i) := 2*cos(x[i]) + 3
13     u2(i) := 3*sin(x[i]) + 5
14
15     INSTRUCTIONS:
16     for i
17         y1[i] = sum([j], A[i, j]*u1(j))
18         y2[i] = sum([j], A[i, j]*u2(j))
19     end i

```

Listing 6. A LoOPY kernel evaluating arrays y1 and y2.

Additionally, LoOPY IR provides a node called a *substitution rule*. These are declared on lines 12–13 of the listing and invoked on lines 17–18. These substitution rules [28] are inlined during code-generation, however, they can be used to implement targeted transformations such as, prefetching the accesses to the substitution rule to a local / private temporary. Klöckner et al. [29] demonstrated this in the context of higher order Finite Element Methods.

In Section 7, we present a specification for storing transformation knowledge for programs that execute einsum operations. In this specification, we use LoOPY both as a descriptive grammar and as a language for specifying transformations. Notably, the contributions in this paper are independent of LoOPY, which is used solely as an IR and a transformation description language for the accompanying implementation.

## B Induced Graph

In this section, we provide a mapping from a batched einsum to a colored graph and a mapping from a colored graph to a batched einsum. In Section 6, we saw that these mappings are fundamental to our batched canonicalization algorithm. Prior to describing our graph constructions corresponding to batched einsums, we provide the definitions of the following terms which will be helpful during the process.

**Definition 19** (All dimensions in an einsum). We define the set of all dimensions for a batched einsum  $e$  as

$$\text{AllDims}(e) = \{\text{Dim}(a) : a \in \mathcal{A}^{\text{all}}(e)\} \cup \{|\mathcal{I}^{\text{out}}(e)|\}.$$

**Definition 20** (Input accesses in an einsum). We define the set of all the input accesses for a batched einsum  $e$  as

$$\text{InputAccesses}(e) = \bigcup_{j=1}^n \left\{ (i, j, \mathcal{I}_d^{\text{in},j}, d) : d \in \{1, \dots, |\mathcal{I}^{\text{in},j}|\}, i \in \{1, 2, \dots, b\}, j \in \{1, 2, \dots, n\} \right\} \quad (3)$$

**Definition 21** (Output accesses in an einsum). We define the set of all the output accesses for a batched einsum  $e$  as

$$\text{OutputAccesses}(e) = \{(I_d^{\text{out}}, d) : d \in \{1, \dots, |\mathcal{I}^{\text{out}}|\}\}.$$

**Definition 22** (All data types in a batched einsum). The set of data types of the inputs in a batched einsum,  $e$ , is given by

$$\text{Dtypes}(e) = \{\text{Dtype}(a) : a \in \mathcal{A}^{\text{all}}(e)\}.$$

**Definition 23** (Axis lengths in a batched einsum). The set of axis lengths in a batched einsum,  $e$ , is given by

$$\text{AxisLengths}(e) = \{(\text{Shape}(a))_i : i \in \{1, \dots, \text{Dim}(a)\}, a \in \mathcal{A}^{\text{all}}(e)\}.$$

**Definition 24** (Induced Graph). A graph induced by a batched einsum  $(N^{\text{IDG}}, \iota_{\text{dtype}}, \iota_{\text{length}}, A^{N^{\text{IDG}} \times N^{\text{IDG}}}, c_{N^{\text{IDG}}})$ , where:

- $N^{\text{IDG}}$  is the number of nodes in the graph
- $A$  is the adjacency matrix of the graph.
- $c$  is the coloring vector of the nodes in the graph.
- $\iota_{\text{dtype}}$  is a mapping from a subset of  $\{1, 2, \dots, N^{\text{IDG}}\}$  to numeric data types.
- $\iota_{\text{length}}$  is a mapping from a subset of  $\{1, 2, \dots, N^{\text{IDG}}\}$  to non-negative integers.

## B.1 Mapping Batched Einsum to Induced Graph

We proceed to outline our construction process for an *induced graph* for a batched einsum  $e$  defined by the tuple  $(b, n, \mathcal{I}^{\text{out}}, (\mathcal{I}^{\text{in},k})_{k=1}^n, ((\mathcal{A}^{j,k})_{k=1}^n)_{j=1}^b)$ . We will use the following notation to simplify our construction process:

- $N_{\text{arg}} = |\mathcal{A}^{\text{all}}(e)|$
- $N_{\text{index}} = |\mathcal{I}^{\text{all}}(e)|$
- $N_{\text{length}} = |\text{AxisLengths}(e)|$
- $N_{\text{dim}} = \max(\text{Dims}(e))$
- $N_{\text{dtype}} = |\text{Dtypes}(e)|$
- $N_{\text{access,in}} = |\text{InputAccesses}(e)|$
- $N_{\text{access,out}} = |\text{OutputAccesses}(e)|$

In this construction, we assign nodes to various components of a batched einsum as follows: one node per argument, one node per index, one node per unique numeric data type of the arrays, one node per unique axis length, one node per index access, one node per dimension index, and one node per output. Consequently, we obtain the number of nodes in the graph as follows:

$$N^{\text{IDG}} = \left( N_{\text{arg}} + N_{\text{index}} + N_{\text{dtype}} + N_{\text{length}} + N_{\text{dim}} + N_{\text{access,in}} + N_{\text{access,out}} + b + n \right) \quad (4)$$

We now define the mappings from the different components of the batched einsum to the node labels in our graph.

- Choose a numbering for the arrays, denoted by the bijective map  $\iota_{\text{arg}} : \{1, 2, \dots, N_{\text{arg}}\} \mapsto \mathcal{A}^{\text{all}}$ .
- Choose a numbering for the indices, denoted by the bijective map  $\iota_{\text{index}} : \{N_{\text{arg}} + 1, \dots, N_{\text{arg}} + N_{\text{index}}\} \mapsto \mathcal{I}^{\text{all}}$ .

- Choose a numbering for the input accesses, denoted by the bijective map  $\iota_{\text{access,in}} : \{N_{\text{arg}} + N_{\text{index}} + 1, \dots, N_{\text{arg}} + N_{\text{index}} + N_{\text{access,in}}\} \mapsto \text{InputAccesses}(e)$ .
- Choose a numbering for the output accesses, denoted by the bijective map  $\iota_{\text{access,out}} : \{N_{\text{arg}} + N_{\text{index}} + N_{\text{access,in}} + 1, \dots, N_{\text{arg}} + N_{\text{index}} + N_{\text{access,in}} + N_{\text{access,out}}\} \mapsto \text{OutputAccesses}(e)$ .
- Choose a numbering for the outputs, denoted by the bijective map  $\iota_{\text{output}} : \{N_{\text{arg}} + N_{\text{index}} + N_{\text{access,in}} + N_{\text{access,out}} + 1, \dots, N_{\text{arg}} + N_{\text{index}} + N_{\text{access,in}} + N_{\text{access,out}} + b\} \mapsto \{1, 2, \dots, b\}$ .
- Choose a numbering for the operand positions, denoted by the bijective map  $\iota_{\text{arg-pos}} : \{N_{\text{arg}} + N_{\text{index}} + N_{\text{access,in}} + N_{\text{access,out}} + b + 1, \dots, N_{\text{arg}} + N_{\text{index}} + N_{\text{access,in}} + N_{\text{access,out}} + b + n\} \mapsto \{1, 2, \dots, n\}$ .
- Choose a numbering for the data types, denoted by the bijective map

$$\begin{aligned} \iota_{\text{dtype}} : \{ & N_{\text{arg}} + N_{\text{index}} + N_{\text{access,in}} + N_{\text{access,out}} + b + n + 1, \\ & \dots, \\ & N_{\text{arg}} + N_{\text{index}} + N_{\text{access,in}} + N_{\text{access,out}} + b + n + N_{\text{dtype}} \} \mapsto \text{Dtypes}(e). \end{aligned} \quad (5)$$

- Choose a numbering for the axis lengths, denoted by the bijective map

$$\begin{aligned} \iota_{\text{length}} : \{ & N_{\text{arg}} + N_{\text{index}} + N_{\text{access,in}} + N_{\text{access,out}} + b + n + N_{\text{dtype}} + 1, \\ & \dots, \\ & N_{\text{arg}} + N_{\text{index}} + N_{\text{access,in}} + N_{\text{access,out}} + b + n + N_{\text{dtype}} + N_{\text{length}} \} \mapsto \text{AxisLengths}(e). \end{aligned} \quad (6)$$

- Choose a numbering for the dimensions of an array, denoted by the bijective map,

$$\begin{aligned} \iota_{\text{dim}} = \{ & (N_{\text{arg}} + N_{\text{index}} + N_{\text{access,in}} + N_{\text{access,out}} + b + n + N_{\text{dtype}} + N_{\text{length}} + i) \mapsto i : \\ & i \in \{1, 2, \dots, N_{\text{dim}}\} \} \end{aligned} \quad (7)$$

We proceed to define specific sets that contribute to the edges in the graph, representing the interactions among various components in  $e$ .

- We define a set of edges to characterize the indexing contribution of an input array to a output. We denote this as  $E_{\text{access,in-to-arg}}$ .

$$E_{\text{access,in-to-arg}} = \left\{ \left( \iota_{\text{access,in}}^{-1} \left( \left( (i, j, \mathcal{I}^{\text{in},j})_d, d \right) \right), \iota_{\text{arg}}^{-1} \left( \mathcal{A}^{i,j} \right) \right) : \right. \right. \\ \left. \left. d \in \{1, \dots, \text{Dim}(\mathcal{A}^{i,j})\}, j \in \{1, \dots, n\}, i \in \{1, \dots, b\} \right\} \right.$$

- We now define edges that characterize an access node i.e. its index, the dimension being indexed over and the output it is contributing to. We denote these as  $E_{\text{arg-pos-to-access,in}}$ ,  $E_{\text{output-to-access,in}}$ ,  $E_{\text{index-to-access,in}}$ , and,  $E_{\text{dim-to-access,in}}$ .

$$E_{\text{arg-pos-to-access,in}} = \{(\iota_{\text{arg-pos}}^{-1}(a), \iota_{\text{access,in}}^{-1}((j, a, i, k))) : (j, a, i, k) \in \text{InputAccesses}(e)\} \quad (8)$$

$$E_{\text{output-to-access,in}} = \{(\iota_{\text{output}}^{-1}(i), \iota_{\text{access,in}}^{-1}((j, a, i, k))) : (j, a, i, k) \in \text{InputAccesses}(e)\} \quad (9)$$

$$E_{\text{index-to-access,in}} = \{(\iota_{\text{index}}^{-1}(j), \iota_{\text{access,in}}^{-1}((j, a, i, k))) : (j, a, i, k) \in \text{InputAccesses}(e)\} \quad (10)$$

$$E_{\text{dim-to-access,in}} = \{(\iota_{\text{dim}}^{-1}(k), \iota_{\text{access,in}}^{-1}((j, a, i, k))) : (j, a, i, k) \in \text{InputAccesses}(e)\} \quad (11)$$

- We now define edges that characterize an output indexing node. We denote these as  $E_{\text{index-to-access,out}}$ , and,  $E_{\text{dim-to-access,out}}$ .

$$E_{\text{index-to-access,out}} = \{(\iota_{\text{index}}^{-1}(i), \iota_{\text{access,out}}^{-1}((i, d))) : (i, d) \in \text{OutputAccesses}(e)\} \quad (12)$$

$$E_{\text{dim-to-access,out}} = \{(\iota_{\text{dim}}^{-1}(d), \iota_{\text{access,out}}^{-1}((i, d))) : (i, d) \in \text{OutputAccesses}(e)\} \quad (13)$$

- We introduce edges to characterize the iteration count corresponding to each index. We denote this as  $E_{\text{length}}$ :

$$E_{\text{length}} = \left\{ \left( \iota_{\text{length}}^{-1}((\text{Shape}(\mathcal{A}^{i,k}))_d), \iota_{\text{index}}^{-1}((\mathcal{I}^{\text{in},k})_d) \right) : d \in \{1, \dots, \text{Dim}(\mathcal{A}^{i,k})\}, k \in \{1, \dots, n\}, i \in \{1, \dots, b\} \right\} \quad (14)$$

- We introduce edges to characterize the numeric data type corresponding to each array. We denote this as  $E_{\text{dtype}}$ .

$$E_{\text{dtype}} = \left\{ \left( \iota_{\text{dtype}}^{-1}(\text{Dtype}(a)), \iota_{\text{arg}}^{-1}(a) \right) : a \in \mathcal{A}^{\text{all}}(e) \right\}$$

- We introduce edges to record the difference between the axis length nodes. We denote this as  $E_{\text{lengthranks}}$ .

$$E_{\text{lengthranks}} = \left\{ (\iota_{\text{length}}^{-1}(l_i), \iota_{\text{length}}^{-1}(l_j)) : l_j > l_i, l_i \in \text{AxisLengths}(e), l_j \in \text{AxisLengths}(e) \right\} \quad (15)$$

- We introduce edges to record the difference between the data type nodes. We denote this as  $E_{\text{dtyperanks}}$ .

$$E_{\text{dtyperanks}} = \left\{ \left( \iota_{\text{dtype}}^{-1}(t_i), \iota_{\text{dtype}}^{-1}(t_j) \right) : \begin{array}{l} \text{DtypeRank}(t_j) > \text{DtypeRank}(t_i), \\ t_i \in \text{Dtypes}(e), \\ t_j \in \text{Dtypes}(e) \end{array} \right\} \quad (16)$$

where,  $\text{DTYPERRANK}$  is the mapping  $\{\text{int8} \mapsto 1; \text{int32} \mapsto 2; \text{int64} \mapsto 3; \text{float16} \mapsto 4; \text{float32} \mapsto 5; \text{float64} \mapsto 6; \text{complex64} \mapsto 7; \text{complex128} \mapsto 8\}$ .

- We introduce edges to record the difference between the dimension nodes. We denote this as  $E_{\text{dimranks}}$ .

$$E_{\text{dimranks}} = \left\{ (\iota_{\text{dim}}^{-1}(d_i), \iota_{\text{dim}}^{-1}(d_j)) : d_j > d_i, d_i \in \text{Dims}(e), d_j \in \text{Dims}(e) \right\} \quad (17)$$

Based on these edges, we initialize the adjacency matrix as:

$$A_{ij} = \begin{cases} 1 & \text{if } (i, j) \in E_{\text{access,in-to-arg}} \\ 1 & \text{if } (i, j) \in E_{\text{output-to-access,in}} \\ 1 & \text{if } (i, j) \in E_{\text{arg-pos-to-access,in}} \\ 1 & \text{if } (i, j) \in E_{\text{index-to-access,in}} \\ 1 & \text{if } (i, j) \in E_{\text{dim-to-access,in}} \\ 1 & \text{if } (i, j) \in E_{\text{index-to-access,out}} \\ 1 & \text{if } (i, j) \in E_{\text{dim-to-access,out}} \\ 1 & \text{if } (i, j) \in E_{\text{length}} \\ 1 & \text{if } (i, j) \in E_{\text{dtype}} \\ 1 & \text{if } (i, j) \in E_{\text{lengthranks}} \\ 1 & \text{if } (i, j) \in E_{\text{dtyperanks}} \\ 1 & \text{if } (i, j) \in E_{\text{dimranks}} \\ 0 & \text{otherwise} \end{cases} \quad (18)$$

We define a node coloring based on the type of the node batched einsum entity associated with it.

$$c_i = \begin{cases} 1 & \text{if } i \leq N_{\text{arg}} \\ 2 & \text{if } 0 < (i - N_{\text{arg}}) \leq N_{\text{index}} \\ 3 & \text{if } 0 < (i - N_{\text{arg}} - N_{\text{index}}) \leq N_{\text{access,in}} \\ 4 & \text{if } 0 < (i - N_{\text{arg}} - N_{\text{index}} - N_{\text{access,in}}) \leq N_{\text{access,out}} \\ 5 & \text{if } 0 < (i - N_{\text{arg}} - N_{\text{index}} - N_{\text{access,in}} - N_{\text{access,out}}) \leq b \\ 6 & \text{if } 0 < (i - N_{\text{arg}} - N_{\text{index}} - N_{\text{access,in}} - N_{\text{access,out}} - b) \leq n \\ 7 & \text{if } 0 < (i - N_{\text{arg}} - N_{\text{index}} - N_{\text{access,in}} - N_{\text{access,out}} - b - n) \leq N_{\text{dtype}} \\ 8 & \text{if } 0 < (i - N_{\text{arg}} - N_{\text{index}} - N_{\text{access,in}} - N_{\text{access,out}} - b - n - N_{\text{dtype}}) \leq N_{\text{length}} \\ 9 & \text{if } 0 < (i - N_{\text{arg}} - N_{\text{index}} - N_{\text{access,in}} - N_{\text{access,out}} - b - n - N_{\text{dtype}} - N_{\text{length}}) \leq N_{\text{dim}} \end{cases} \quad (19)$$

Using the construction outlined above, we obtain the induced graph associated with the batched einsum  $e$  as  $G$ . This graph is defined by the tuple  $(N^{IDG}, \iota_{\text{dtype}}, \iota_{\text{lengths}}, A, c)$ , which are defined in Equations (4), (5), (6), (18), and (19), respectively.

**Example 6** (Induced Graph). For the einsum  $(1, 2, (i), ((ik), (ij)), ((A, B)))$ , with  $\text{Shape}(A) = \text{Shape}(B) = (72, 18)$  and  $\text{Dtype}(A) = \text{Dtype}(B) = \text{F64}$ , we obtain the induced graph as shown in Figure 7. It is worth noting that the nodes corresponding to  $j$  and  $k$  form a part of an automorphism in the graph.

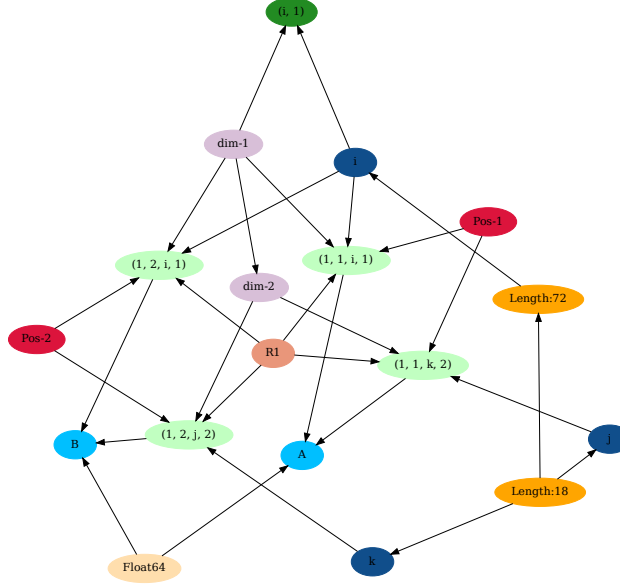


Fig. 7. Induced graph for the batched einsum of Example 6.

## B.2 Reconstructing a Batched Einsum from an Induced Graph

In this section, we provide a mapping from  $G$ , an *induced graph* (Definition 24), to a batched einsum. We will consider that  $G$  is defined by the tuple  $(N^{\text{IDG}}, \iota_{\text{dtype}}, \iota_{\text{lengths}}, A^{N^{\text{IDG}} \times N^{\text{IDG}}}, c_{N^{\text{IDG}}})$  and provide a construction of a batched einsum. The aim of this section is to invert the construction of Section B.1.

Before discussing the construction process, it is important to note that not all induced graphs can be mapped to a valid batched einsum. An example of a non-compliant graph is one that contains a node with a color value of 12, as it violates the condition specified in Equation (19).

We now introduce some terms that will be instrumental in our proposed construction.

- We invert the coloring mapping of Equation (19), to obtain the following sets:

$$\begin{aligned}
 V_{\text{arg}} &= \{i : i \in \{1, \dots, N^{\text{IDG}}\}, c_i = 1\} \\
 V_{\text{index}} &= \{i : i \in \{1, \dots, N^{\text{IDG}}\}, c_i = 2\} \\
 V_{\text{access,in}} &= \{i : i \in \{1, \dots, N^{\text{IDG}}\}, c_i = 3\} \\
 V_{\text{access,out}} &= \{i : i \in \{1, \dots, N^{\text{IDG}}\}, c_i = 4\} \\
 V_{\text{output}} &= \{i : i \in \{1, \dots, N^{\text{IDG}}\}, c_i = 5\} \\
 V_{\text{arg-pos}} &= \{i : i \in \{1, \dots, N^{\text{IDG}}\}, c_i = 6\} \\
 V_{\text{dtype}} &= \{i : i \in \{1, \dots, N^{\text{IDG}}\}, c_i = 7\} \\
 V_{\text{length}} &= \{i : i \in \{1, \dots, N^{\text{IDG}}\}, c_i = 8\} \\
 V_{\text{dims}} &= \{i : i \in \{1, \dots, N^{\text{IDG}}\}, c_i = 9\}
 \end{aligned} \tag{20}$$

– We define the neighbor relations in the graph  $G$ , as:

$$\begin{aligned} \text{Succs}(i) &= \{j : j \in \{1, \dots, N^{\text{IDG}}\}, A_{ij} = 1\} \\ \text{Preds}(i) &= \{j : j \in \{1, \dots, N^{\text{IDG}}\}, A_{ji} = 1\} \end{aligned} \quad (21)$$

The conditions required to invert the construction of Section B.1 consist of:

(C1) For all  $i \in \{1, \dots, n\}$ ,  $c_i$  must belong to  $\{1, \dots, 9\}$ .

(C2) An argument node must not have any successors

$$i \in V_{\text{arg}} \Rightarrow \text{Succs}(i) = \emptyset.$$

(C3) A predecessor of an argument node must either be an input access node or a data type node

$$i \in V_{\text{arg}} \Rightarrow \text{Preds}(i) \subseteq (V_{\text{access,in}} \cup V_{\text{dtype}}).$$

(C4) An argument node must have exactly one data type node as predecessor

$$n \in V_{\text{arg}} \Rightarrow |\text{Preds}(n) \cap V_{\text{dtype}}| = 1.$$

(C5) A data type node can have only other data type nodes as predecessors

$$i \in V_{\text{dtype}} \Rightarrow \text{Preds}(i) \subset V_{\text{dtype}}.$$

(C6) A successor of a data type node must either be an argument node or a data type node

$$i \in V_{\text{dtype}} \Rightarrow \text{Succs}(i) \subseteq V_{\text{arg}} \cup V_{\text{dtype}}.$$

(C7) A successor of an input access node must be an argument node

$$i \in V_{\text{access,in}} \Rightarrow \text{Succs}(i) \subseteq V_{\text{arg}}.$$

(C8) An input access node must have exactly four predecessors, an index node, a dimension node, an argument position node and an output, i.e.

$$\begin{aligned} i \in V_{\text{access,in}} &\Rightarrow |\text{Preds}(i)| = 4 \\ i \in V_{\text{access,in}} &\Rightarrow |\text{Preds}(i) \cap V_{\text{arg-pos}}| = 1 \\ i \in V_{\text{access,in}} &\Rightarrow |\text{Preds}(i) \cap V_{\text{index}}| = 1 \\ i \in V_{\text{access,in}} &\Rightarrow |\text{Preds}(i) \cap V_{\text{output}}| = 1 \\ i \in V_{\text{access,in}} &\Rightarrow |\text{Preds}(i) \cap V_{\text{dim}}| = 1 \end{aligned} \quad (22)$$

(C9) A successor of an output node must be an input access node

$$i \in V_{\text{output}} \Rightarrow \text{Succs}(i) \subseteq V_{\text{access,in}}.$$

(C10) An output node must not have any predecessors

$$i \in V_{\text{output}} \Rightarrow \text{Preds}(i) = \emptyset.$$

(C11) An output access node must not have any successors.

$$i \in V_{\text{access,out}} \Rightarrow \text{Succs}(i) = \emptyset$$

(C12) An output access node must have exactly two predecessors, an index node, and, a dimension node

$$\begin{aligned} i \in V_{\text{access,out}} &\Rightarrow |\text{Preds}(i)| = 2 \\ i \in V_{\text{access,out}} &\Rightarrow |\text{Preds}(i) \cap V_{\text{index}}| = 1 \\ i \in V_{\text{access,in}} &\Rightarrow |\text{Preds}(i) \cap V_{\text{dim}}| = 1 \end{aligned} \quad (23)$$

(C13) A successor of an index node must either be an input access node or an output access node

$$i \in V_{\text{index}} \Rightarrow \text{Succs}(i) \subseteq (V_{\text{access,in}} \cup V_{\text{access,out}}).$$

(C14) An index node must have exactly one node as predecessor. Furthermore, that predecessor must be an index length node.

$$i \in V_{\text{index}} \Rightarrow |\text{Preds}(i)| = 1 \text{ and } |\text{Preds}(i) \cap V_{\text{length}}| = 1.$$

(C15) A predecessor of an axis length node must be an axis length node

$$i \in V_{\text{length}} \Rightarrow \text{Preds}(i) \subseteq V_{\text{length}}$$

(C16) A successor of an axis length node must either be an index node or an axis length node

$$i \in V_{\text{length}} \Rightarrow \text{Succs}(i) \subseteq (V_{\text{index}} \cup V_{\text{length}}).$$

(C17) A predecessor of a dimension node must be a dimension node

$$i \in V_{\text{dim}} \Rightarrow \text{Preds}(i) \subseteq V_{\text{dim}}.$$

(C18) A successor of a dimension node must either be an access node or a dimension node

$$i \in V_{\text{dim}} \Rightarrow \text{Succs}(i) \subseteq (V_{\text{access,in}} \cup V_{\text{access,out}} \cup V_{\text{dim}}).$$

(C19) An argument position node must not have any predecessors

$$i \in V_{\text{arg-pos}} \Rightarrow \text{Preds}(i) = \emptyset.$$

(C20) A successor of an argument position node must be an input access node

$$i \in V_{\text{arg-pos}} \Rightarrow \text{Succs}(i) \subseteq V_{\text{access,in}}.$$

(C21) The subgraph of  $G$  obtained by retaining only the dimension nodes and the corresponding edges must be a transitive tournament. Equivalently, there exists an ordering  $v_1, \dots, v_n$  of the vertices in  $V_{\text{dim}}$  such that

$$v_j \in \text{Succs}(v_i) \text{ if and only if } i < j.$$

These conditions mirror the edges outlined in the previous section, which correspond to the ranking of nodes across different dimensions as specified in (17).

(C22) The subgraph of  $G$  obtained by retaining only the length nodes and the corresponding edges must be a transitive tournament. Equivalently, there exists an ordering  $v_1, \dots, v_n$  of the vertices in  $V_{\text{length}}$  such that

$$v_j \in \text{Succs}(v_i) \text{ if and only if } i < j.$$

These conditions capture the edges outlined in the previous section, which correspond to the ranking of nodes across axis lengths as specified in (15).

(C23) The subgraph of  $G$  obtained by retaining only the data type nodes and the corresponding edges must be a transitive tournament. Equivalently, there exists an ordering  $v_1, \dots, v_n$  of the vertices in  $V_{\text{dtype}}$  such that

$$v_j \in \text{Succs}(v_i) \text{ if and only if } i < j.$$

These conditions capture the edges outlined in the previous section, which correspond to the ranking of nodes across different numeric data types as specified in (16).

(C24) If  $n_1 \in V_{\text{access,in}}$ ,  $n_2 \in V_{\text{access,in}}$ ,  $i_1 \in \text{Preds}(n_1) \cap V_{\text{index}}$ ,  $i_2 \in \text{Preds}(n_2) \cap V_{\text{index}}$ ,  $(\text{Succs}(n_1) \cap V_{\text{arg}} = \text{Succs}(n_2) \cap V_{\text{arg}}) \wedge (\text{Preds}(n_1) \cap V_{\text{dim}} = \text{Preds}(n_2) \cap V_{\text{dim}})$ , then  $\text{Preds}(i_1)$  must be equal to  $\text{Preds}(i_2)$ . This enforces that the arrays being of consistent shape by the following condition.

(C25) If  $n \in V_{\text{access,out}}$ ,  $i \in \text{Preds}(n) \cap V_{\text{index}}$ , then  $\text{Succs}(i) \cap V_{\text{access,in}}$  must be non-empty. This enforces that if an index node is indexing an output node then the index node is seen in one of the input nodes as well.

(C26) If  $n \in V_{\text{access,in}}$ ,  $i \in \text{Preds}(n) \cap V_{\text{index}}$ ,  $d \in \text{Preds}(n) \cap V_{\text{dim}}$ ,  $k \in \text{Preds}(n)$  and  $k \in V_{\text{arg-pos}}$ , then for all  $o \in V_{\text{output}}$ , the set  $\{n' \in V_{\text{access,in}} : \{i, d, k, o\} \subseteq \text{Preds}(n')\}$  must be singleton. This condition enforces that the input indexing must be consistent for all outputs.

(C27) The set  $\{\text{Preds}(n) \cap V_{\text{index}} : n \in V_{\text{access,out}}\}$  must have dimensionality of  $|V_{\text{access,out}}|$ . This condition enforces that all output indices are distinct.

(C28) For all  $k \in V_{\text{arg-pos}}$ ,  $o \in V_{\text{output}}$ ,  $\text{Acc}_{k,o} = \{n : k \in \text{Preds}(n), o \in \text{Preds}(n), n \in V_{\text{access,in}}\}$ . Then, the set  $\left( \bigcup_{a \in \text{Acc}_{k,o}} \text{Succs}(a) \right)$  must be singleton.  
This condition stipulates that only a single argument is indexed for an output.

(C29) For all  $k \in V_{\text{arg-pos}}$ ,  $o \in V_{\text{output}}$ , if  $\text{Acc}_{k,o} = \{n : n \in V_{\text{access,in}}, k \in \text{Preds}(n), o \in \text{Preds}(n)\}$ , and  $\text{Dims}_{k,o} = \bigcup_{n \in \text{Acc}_{k,o}} \text{Preds}(n) \cap V_{\text{dim}}$ , then, the following conditions must hold:

$$|\{d : d \in \text{Dims}_{k,o}, \text{Preds}(d) \cap V_{\text{dim}} = \emptyset\}| = 1$$

$$|\{d : d \in \text{Dims}_{k,o}, \text{Preds}(d) \cap \text{Dims}_{k,o} \neq \emptyset\}| = |\text{Dims}_{k,o}| - 1$$

This condition enforces that all consecutive dimensions of an argument are indexed.

(C30) We define  $\text{Dims}_{\text{out}} = \bigcup_{n \in V_{\text{access,out}}} \text{Preds}(n) \cap V_{\text{dim}}$ . Then,

$$|\{d : d \in \text{Dims}_{\text{out}}, \text{Preds}(d) \cap V_{\text{dim}} = \emptyset\}| = 1$$

$$|\{d : d \in \text{Dims}_{\text{out}}, \text{Preds}(d) \cap \text{Dims}_{\text{out}} \neq \emptyset\}| = |\text{Dims}_{\text{out}}| - 1$$

This condition enforces that all consecutive dimensions of the output are indexed.

**REMARK 2.** Our induced graph construction from Section B.1 satisfies the properties (C1)–(C30).

For an induced graph that satisfies the compliance properties mentioned above, we can obtain its corresponding batched einsum by following these steps:

**Step 1.** Choose two functions  $\text{IndexName} : \mathbb{Z}^+ \rightarrow \text{identifier}$ , for naming an index in the reconstructed batched einsum and  $\text{ArgName} : \mathbb{Z}^+ \rightarrow \text{identifier}$ , for naming an argument in the reconstructed batched einsum.

**Step 2.** Define a mapping for argument ordering in the reconstructed batched einsum, denoted as  $\iota_{\text{arg-pos}}^{\text{inferred}} : V_{\text{arg-pos}} \mapsto \{1, \dots, |V_{\text{arg-pos}}|\}$  such that if  $n_1, n_2 \in V_{\text{dim}}$  and  $n_1 < n_2$ , then  $\iota_{\text{arg-pos}}^{\text{inferred}}(n_1) < \iota_{\text{arg-pos}}^{\text{inferred}}(n_2)$ .

**Step 3.** Define a mapping for the output ordering in the reconstructed batched einsum, denoted as  $\iota_{\text{output}}^{\text{inferred}} : V_{\text{output}} \mapsto \{1, \dots, |V_{\text{output}}|\}$  such that if  $n_1, n_2 \in V_{\text{output}}$  and  $n_1 < n_2$ , then  $\iota_{\text{output}}^{\text{inferred}}(n_1) < \iota_{\text{output}}^{\text{inferred}}(n_2)$ .

**Step 4.** Define a mapping for the index symbol ordering in the reconstructed batched einsum, denoted as  $\iota_{\text{index}}^{\text{inferred}} : V_{\text{index}} \mapsto \{1, \dots, |V_{\text{index}}|\}$  such that if  $n_1, n_2 \in V_{\text{index}}$  and  $n_1 < n_2$ , then  $\iota_{\text{index}}^{\text{inferred}}(n_1) < \iota_{\text{index}}^{\text{inferred}}(n_2)$ .

**Step 5.** Define a mapping for the argument ordering the reconstructed batched einsum, denoted as  $\iota_{\text{arg}}^{\text{inferred}} : V_{\text{arg}} \mapsto \{1, \dots, |V_{\text{arg}}|\}$  such that if  $n_1, n_2 \in V_{\text{arg}}$  and  $n_1 < n_2$ , then  $\iota_{\text{arg}}^{\text{inferred}}(n_1) < \iota_{\text{arg}}^{\text{inferred}}(n_2)$ .

**Step 6.** Define the mapping for the dimensions in the reconstructed batched einsum,  $\iota_{\text{dim}}^{\text{inferred}} : V_{\text{dim}} \mapsto \{1, \dots, |V_{\text{dim}}|\}$ , as:

$$\iota_{\text{dim}}^{\text{inferred}}(n) = 1 + |\text{Preds}(n) \cap V_{\text{dim}}|. \quad (24)$$

**Step 7.** Find the output index, denoted by  $\mathcal{I}^{\text{out,inferred}}$ , as:

$$\mathcal{I}^{\text{out,inferred}} = \text{IndexName} \left( \iota_{\text{index}}^{\text{inferred}}(\text{OutIndex}(k)) \right) \quad (25)$$

where,

$$\text{OutIndex}(k) \in \left\{ i : \left( \iota_{\text{dim}}^{\text{inferred}} \right)^{-1}(k) \in \text{Preds}(n), n \in V_{\text{access,out}} \right\}. \quad (26)$$

From the criterion in equation (23), we can see the there is exactly one solution for  $\text{OutIndex}(k)$  in the above equation (26).

**Step 8.** Find the argument dimensions, denoted by  $\text{ArgDim}(k)$ , as:

$$\text{ArgDim}(k) = \left| \left\{ d \in V_{\text{dim}} : \left\{ d, \left( \iota_{\text{arg-pos}}^{\text{inferred}} \right)^{-1}(k) \right\} \subset \text{Preds}(a), a \in V_{\text{access,in}} \right\} \right| \quad (27)$$

**Step 9.** Find the input index list, denoted by  $\mathcal{I}^{\text{in,inferred}}$ , as:

$$\mathcal{I}^{\text{in,inferred}} = \left( \left( \text{IndexName} \left( \iota_{\text{index}}^{\text{inferred}}(\text{InputIndex}(d, j)) \right) \right)_{d=1}^{\text{ArgDim}(j)} \right)_{j=1}^{|V_{\text{arg-pos}}|} \quad (28)$$

where,

$$\begin{aligned} \text{InputIndex}(d, j) \in & \left\{ i : i \in \text{Preds}(n), \right. \\ & i \in V_{\text{index}}, \\ & \left. \left\{ \left( \iota_{\text{arg-pos}}^{\text{inferred}} \right)^{-1}[j], \left( \iota_{\text{dim}}^{\text{inferred}} \right)^{-1}[d] \right\} \subset \text{Preds}(n), \right. \\ & n \in V_{\text{access,in}} \} \end{aligned} \quad (29)$$

From the criterion in equation (22), we can see the there is exactly one solution for  $\text{InputIndex}(d, j)$  in the above equation (29).

**Step 10.** Find the argument sequences as  $\left( (\mathcal{A}^{i,j,\text{inferred}})_{j=1}^{|V_{\text{arg-pos}}|} \right)_{i=1}^{|V_{\text{output}}|}$ , where  $\mathcal{A}^{i,j,\text{inferred}}$  is an array with the symbol  $\text{ArgName} \left( \iota_{\text{array}}^{\text{inferred}}(\text{ArgLabel}(i, j)) \right)$ , with the shape  $(\iota_{\text{length}}(\text{LengthLabel}(i, j)))_{j=1}^{\text{ArgDim}(j)}$  and with the data type  $\iota_{\text{dtype}}(\text{DtypeLabel}(i, j))$ , where,

$$\begin{aligned}
 \text{ArgLabel}(i, j) \in \{a : & \{ \left( \begin{smallmatrix} \text{inferred} \\ \text{output} \end{smallmatrix} \right)^{-1}(i), \right. \\
 & \left. \left( \begin{smallmatrix} \text{inferred} \\ \text{arg-pos} \end{smallmatrix} \right)^{-1}(j) \} \subset \text{Preds}(n), \\
 & n \in (\text{Preds}(n) \cap V_{\text{access,in}}), \\
 & a \in V_{\text{arg}} \}
 \end{aligned} \tag{30}$$

$$\text{DtypeLabel}(i, j) \in \{d : V_{\text{dtype}}, d \in \text{Preds}(\text{ArgLabel}(i, j))\} \tag{31}$$

$$\text{LengthLabel}(i, j) \in \{l : l \in V_{\text{length}}, l \in \text{Preds}(\text{InputIndex}(i, j))\} \tag{32}$$

From the criteria (C28), (C4), and, (C14), we can see that the equations (30), (31), and, (32) have exactly one solution.

**Step 11.** Using the previous steps, we reconstruct our batched einsum as a batched einsum defined by the tuple  $(|V_{\text{output}}|, |V_{\text{arg-pos}}|, \mathcal{I}^{\text{out,inferred}}, (\mathcal{I}^{k,\text{in,inferred}})_{i=1}^{|V_{\text{arg-pos}}|}, (\mathcal{A}^{i,j,\text{inferred}})_{j=1}^{|V_{\text{arg-pos}}|})_{i=1}^{|V_{\text{output}}|}$ .

### C DG-FEM Batched Einsum Kernel Patterns

```

1  jac(f, e)      := J[f, e]
2  mat(i, f, j)  := D[i, f, j]
3  f1(f, e, j)   := F_1[f, e, j]
4  f2(f, e, j)   := F_2[f, e, j]
5  # ...
6  fb(f, e, j)   := F_b[f, e, j]
7
8  for iel, idof
9    y1[iel, idof] = sum([iface, jdof], f1(iface, iel, jdof)
10                          * jac(iface, jdof)
11                          * mat(idof, iface, jdof)))
12    y2[iel, idof] = sum([iface, jdof], f2(iface, iel, jdof)
13                          * jac(iface, jdof)
14                          * mat(idof, iface, jdof)))
15  # ...
16    yb[iel, idof] = sum([iface, jdof], fb(iface, iel, jdof)
17                          * jac(iface, jdof)
18                          * mat(idof, iface, jdof)))
19  end iel, idof

```

Listing 7. A kernel performing  $b$ -applications of the face-mass operation. The variables  $F_1, \dots, F_b$  correspond to the surface fluxes.  $\text{jac}$  is the substitution rule corresponding to the Jacobian terms and  $\text{mat}$  is the rule corresponding to the tabulated reference surface integral.

```

1  jac(x, r, e)  := J[x, r, e]

```

```

2  mat(r,i,j) := D[r,i,j]
3  f1(x,e,j)  := u1[e, j] if x == 0 else (v1[e, j] if x == 1 else w1[e, j])
4  f2(x,e,j)  := u2[e, j] if x == 0 else (v2[e, j] if x == 1 else w2[e, j])
5  # ...
6  fb(x,e,j)  := ub[e, j] if x == 0 else (vb[e, j] if x == 1 else wb[e, j])
7
8  for iel, idof
9    y1[iel,idof] = sum([itopo_dim,iambient_dim,jdof], f1(itopo_dim,iel,jdof)
10                           * jac(itopo_dim,iambient_dim,iel)
11                           * mat(iambient_dim,idof,jdof)))
12    y2[iel,idof] = sum([itopo_dim,iambient_dim,jdof], f2(itopo_dim,iel,jdof)
13                           * jac(itopo_dim,iambient_dim,iel)
14                           * mat(iambient_dim,idof,jdof)))
15  # ...
16    yb[iel,idof] = sum([itopo_dim,iambient_dim,jdof], fb(itopo_dim,iel,jdof)
17                           * jac(itopo_dim,iambient_dim,iel)
18                           * mat(iambient_dim,idof,jdof)))
19 end iel, idof

```

Listing 8. A kernel performing  $b$ -applications of the local divergence operation. The tuples  $\{(u1, v1, w1), \dots, (ub, vb, wb)\}$  correspond to the individual components of the input vector fields.  $\text{jac}$  is the substitution rule corresponding to the Jacobian terms and  $\text{mat}$  is the reference derivative matrix.

```

1  jac(x,r,e) := J[x,r,e]
2  mat(r,i,j) := D[r,i,j]
3  f1(x,e,j)  := u1[e, j]
4  f2(x,e,j)  := u2[e, j]
5  # ...
6  fb(x,e,j)  := ub[e, j]
7
8  for iel, idof
9    y1[itopo_dim, iel,idof] = sum([iambient_dim,jdof], f1(iel,jdof)
10                           * jac(itopo_dim,iambient_dim,iel)
11                           * mat(iambient_dim,idof,jdof)))
12    y2[itopo_dim, iel,idof] = sum([iambient_dim,jdof], f2(iel,jdof)
13                           * jac(itopo_dim,iambient_dim,iel)
14                           * mat(iambient_dim,idof,jdof)))
15  # ...
16    yb[itopo_dim, iel,idof] = sum([iambient_dim,jdof], fb(iel,jdof)
17                           * jac(itopo_dim,iambient_dim,iel)
18                           * mat(iambient_dim,idof,jdof)))

```

19 **end iel, idof**

Listing 9. A kernel performing  $b$ -applications of the local gradient operation. The variables  $\{u_1, \dots, u_b\}$ , correspond to the input scalar fields.  $\text{jac}$  is the substitution rule corresponding to the Jacobian terms and  $\text{mat}$  is the reference derivative matrix.